TOOLS AND RESOURCES

Novel human cell expression method reveals the role and prevalence of posttranslational modification in non-muscle tropomyosins

Peter J. Carman[1,2], Kyle R. Barrie[1,2], Roberto Dominguez[1,*]

[1] Department of Physiology, Perelman School of Medicine, University of Pennsylvania, Philadelphia, PA, 19104, USA

[2] Biochemistry and Molecular Biophysics Graduate Group, Perelman School of Medicine, University of Pennsylvania, Philadelphia, PA, 19104, USA

* Correspondence: droberto@pennmedicine.upenn.edu

Abstract

Biochemical studies require large protein quantities, which are typically obtained using bacterial expression. However, the folding machinery of bacteria is inadequate for many mammalian proteins, which additionally undergo posttranslational modifications (PTMs) that bacteria, yeast, or insect cells cannot perform. Many proteins also require native N- and C-termini and cannot tolerate extra tag amino acids for function. Tropomyosin, a coiled coil that decorates most actin filaments in cells, requires both native N- and C-termini and PTMs, specifically N-terminal acetylation, to polymerize along actin filaments. Here, we describe a new method that combines native protein expression in human cells with an intein-based purification tag that can be precisely removed after purification. Using this method, we expressed several non-muscle tropomyosin isoforms. Mammalian cell-expressed tropomyosins are functionally different from their *E. coli*-expressed counterparts, display multiple types of PTMs, and can form heterodimers. This method can be extended to other proteins, as demonstrated here for α-synuclein.

Introduction

Biochemical and structural studies require large amounts of pure proteins and protein complexes. When these cannot be purified from natural sources, scientists typically opt for protein expression in bacteria, and N- or C-terminal affinity tags are commonly used for protein purification. These tags are often left on proteins during subsequent studies and, when they are enzymatically removed, extra amino acids often remain (1). While these approaches have proven powerful and will likely continue to be used in the future, there are many circumstances in which they fail to produce accurate results. For example, most human proteins undergo multiple types of posttranslational modifications (PTMs), including acetylation, phosphorylation, and methylation (2). Such PTMs play crucial roles in the regulation of protein function, including protein stability, protein-protein interactions, and enzymatic activity (3-6). Most PTMs present in human proteins cannot be processed by expression systems such as bacteria, yeast, or insect cells (7-12). These expression systems may also lack the adequate machinery to fold certain mammalian proteins (13-16). Many proteins also require native N- and C-termini and cannot tolerate the presence of extra amino acids from purification tags for proper function (17-21). We were confronted with these problems while studying tropomyosin (Tpm), a protein of central importance in the actin cytoskeleton (22).

Tpm is a coiled coil dimer that polymerizes head-to-tail to form two contiguous chains on opposite sides of the actin filament (F-actin). Through alternative splicing of four different genes (*TPM1-4*), up to 40 distinct Tpm isoforms can be produced, of which ~30 have been detected as proteins (23). Most isoforms are ~280-amino acids long (called long isoforms), comprising seven pseudo-repeats of ~40 amino acids, with each pseudo-repeat spanning the length of one actin subunit along the long-pitch helix of the actin filament. Long Tpm isoforms decorate the contractile actin filaments of muscle cells. In non-muscle cells, the majority of actin filaments are also decorated with Tpm (24). Some of the non-muscle Tpm isoforms lack exon 2 and as a consequence are one pseudo-repeat shorter (called short isoforms). Because the six human actin isoforms are very similar, sharing 93–99% sequence identity, it has been proposed that the decoration of actin filaments with distinct Tpm isoforms provides a mechanism for filaments to assume different identities and become functionally segregated in cells (25). Tpm can move azimuthally on actin, helping to regulate the interactions of most actin-binding proteins, including myosin (26,27).

Although there is high sequence similarity among Tpm isoforms, gene knockout and isoform overexpression studies have shown that they play non-redundant roles (22). For example, Tpm4.2 knockout causes low platelet count (28), whereas Tpm3.5 knockout causes softer, less mechanically resilient lenses in the eye (29), indicating that other Tpm isoforms cannot compensate for the lack of Tpm4.2 or Tpm3.5. Similarly, different Tpm isoforms have been implicated in processes such as muscle contraction (30,31), cytokinesis (32,33), embryogenesis (34,35), and endocytosis (36). The temporal expression of Tpm isoforms is also tightly controlled. Thus, sixteen isoforms are up- or down-regulated at different stages of brain development in rodents (37,38). Tpm3.1 and Tpm3.2 are found in the axon in developing neurons, whereas in mature neurons they are expressed only in cell bodies and replaced in axons by Tpm1.12 and Tpm4.2 (39).

PTMs, and in particular N-terminal acetylation (Nt-acetylation) (40-42) and phosphorylation (43-46), have been shown to critically regulate Tpm function. Proper head-to-tail assembly of Tpm coiled coils along actin filaments requires native N- and C-termini, i.e. free of extra amino acids from tags and Nt-acetylated (40,47), whereas the phosphorylation state of Tpm can also modulate the stiffness and affinity of the head-to-tail interaction as well as the F-actin binding affinity (43,44,46). Despite the importance of these factors, previous biochemical studies have focused on one or two Tpm isoforms purified from muscle or *E. coli*-expressed full-length and peptide fragments of Tpm isoforms that lack PTMs and native N and C-termini. While extra amino acids have been added at the N-terminus to substitute for Nt-acetylation (40,41,48,49), it is unclear how precisely this approach mimics acetylation. Tpm coexpression with the yeast acetyltransferase NatB in *E. coli* has been also used to acetylate the N-terminus (50). However, while yeast NatB can acetylate the N-terminus, the extent of this modification varies for different Tpm isoforms, being as low as 30% for certain mammalian Tpm isoforms, whereas other types of PTMs are not accounted for (8). Furthermore, as we show here, the initiator methionine of many Tpm isoforms must be removed by mammalian N-terminal aminopeptidases, and Nt-acetylation occurs on the second residue, which this approach can also not account for (51).

Here, we describe a method that combines expression in human Expi293F cells, which grow in suspension to high density and contain the native PTM machinery, with an intein-based affinity tag that can be precisely removed through self-cleavage after purification. We applied this method to the expression of six Tpm isoforms. We demonstrate the general applicability of this method to other proteins by also showing expression of α-synuclein, a protein implicated in several neurodegenerative disorders whose function is critically regulated by numerous PTMs

(52,53). We characterize the expressed proteins, including a functional analysis of the expressed Tpm isoforms in comparison with their *E. coli*-expressed counterparts, and a comprehensive analysis of PTMs using proteomics analysis. We finally show that non-muscle Tpm isoforms can form heterodimers *in vitro* and in cells, as previously shown for muscle isoforms purified from tissues.

Results

Human cell expression and intein-mediated purification method and its application to Tpm and α-synuclein

The expression method developed here combines mammalian cell expression with a self-cleavable affinity tag. The cells used are Expi293F, commercialized by Thermo Fisher Scientific, which are based on human embryonic kidney (HEK) cells and have been adapted to grow in suspension to high density (54,55). These cells can be transiently transfected, display high protein expression levels, and have the endogenous protein folding and PTM machineries necessary for native expression and modification of human proteins. The self-cleavable affinity tag consists of a modified intein element followed by a chitin-binding domain (CBD), and is based on the IMPACT (intein-mediated purification with an affinity chitin-binding tag) system marketed by New England Biolabs (56,57). Both, N- and C-terminal intein-CBD tags are commercially available for bacterial protein expression, but we opted here to use a C-terminal intein-CBD tag for expression in mammalian cells to allow for N-terminal processing and acetylation, which affects ~90% of human proteins (58). After purification on the high-affinity chitin resin, self-cleavage of the intein takes place precisely after the last endogenous amino acid of the expressed target protein, leaving no extra amino acids from the tag. While both mammalian cell expression (59-61) and intein-CBD purification tags (62) have been previously used, to our knowledge this is the first time that the two are combined in a single method. Self-cleavage of the intein is thiol-catalyzed, meaning that a portion of the intein of bacterial origin is prematurely activated in the reducing environment of the cytoplasm of eukaryotic cells, likely explaining why they have not been used for mammalian cell expression.

We built a new vector (named pJCX4), which incorporates the *Mxe* GyrA intein and CBD into a mammalian-cell expression vector (*Figure 1A*). The *Mxe* GyrA intein is a 198-amino acid self-splicing protein from *Mycobacterium xenopi* (63). In its native form, the intein catalyzes its own excision from the precursor protein, forming a new peptide bond between the N- and C-terminal fragments that flank the intein (64,65). To harness this process for expression and purification of a target protein, the N- and C-terminal fragments of the intein precursor protein are substituted respectively by the target protein and the CBD affinity tag, and two amino acids at the C-terminus of the intein moiety (Asn-Cys) are mutated to Ala-Thr, which turns the intein splicing activity into precise cleavage at the junction between the target protein and the intein (66).

In addition to the intein-CBD element, the expression vector includes the cytomegalovirus promoter (CMV) and the simian virus 40 (SV40) polyadenylation (polyA) signal, as well as the woodchuck hepatitis virus posttranscriptional regulatory element (WPRE) for enhanced expression (*Figure 1A*). It also includes pUC and f1 origins of replication for propagation in *E. coli* and the SV40 origin of replication for propagation in mammalian cells. Finally, the vector contains the kanamycin resistance gene for selection in bacteria. These elements collectively allow for plasmid cloning and amplification in *E. coli* and expression in Expi293F cells. A number of restriction sites are available to clone the 5' end of a target gene, while the SapI or SpeI sites must be used to clone the 3' end, to ensure that no vector- or tag-derived amino acids remain

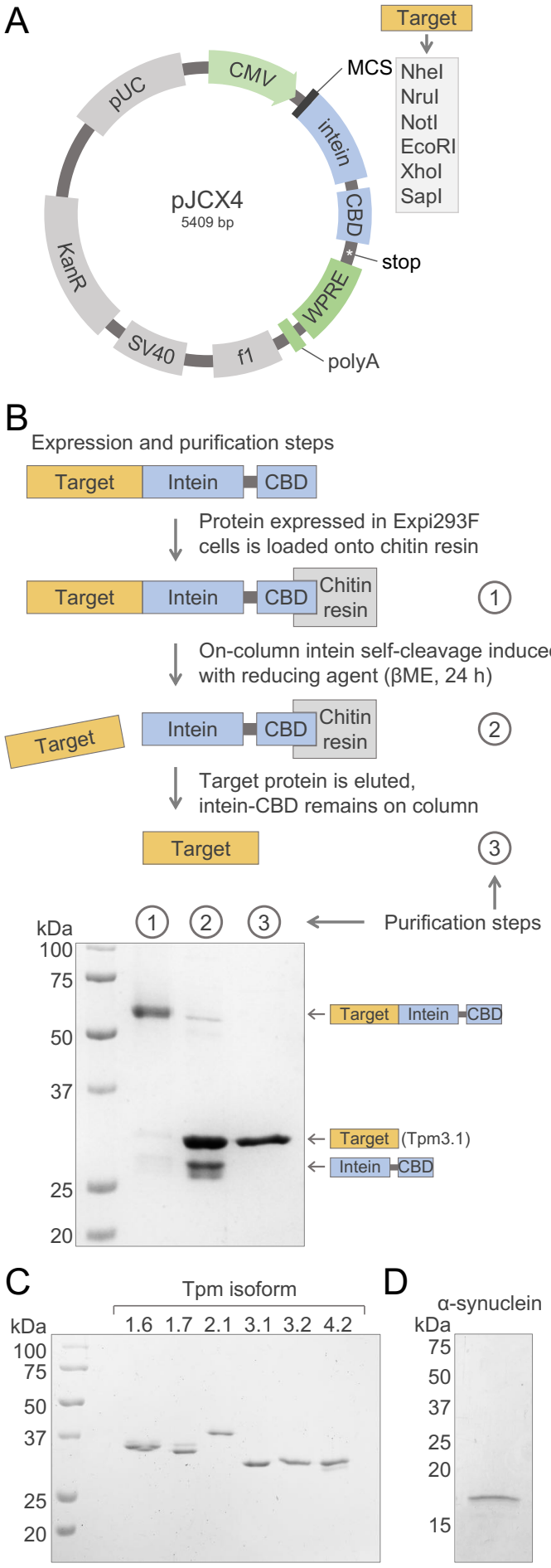

Figure 1. Cloning, expression and purification of Tpm isoforms and α-synuclein in Expi293F cells. (A) Schematic representation of the mammalian-cell expression vector designed here, featuring an intein-CBD affinity-purification and self-cleavage element. Cloning into this vector results in the expression of the target protein as a fusion protein with intein-CBD (see also *Figure S1*). (B) Schematic representation of the expression and purification steps, including purification on a chitin resin of the protein expressed in Expi293F cells, thiol-catalyzed self-cleavage of the intein (using β-mercaptoethanol or βME), and elution of the target protein. As an example, SDS-PAGE analysis at the bottom of the panel illustrates the progression of these steps for Tpm3.1 (see also *Figure S1*). (C and D) SDS-PAGE analysis and Coomassie Brilliant Blue R-250 (BIO-RAD) staining of the six Tpm isoforms (panel C) and α-synuclein (panel D) expressed and purified using this strategy, and further purified using ion exchange chromatography (see Materials and methods).

B

General cloning strategy

Direction	Restriction site	Sequence
Forward (5') primer (option 1):	NotI	5'- TT CGC GGC CGC GCC ACC NNN NNN … -3'
Forward (5') primer (option 2):	EcoRI	5'- TTC GAA TTC GCC ACC NNN NNN … -3'
Reverse (3') primer (option 1)	SapI	5'- GGT TGC TCT TCC AAC NNN NNN … -3'
Reverse (3') primer (option 2)	SpeI	5'- TT CAC TAG TGC ATC TCC CGT GAT GCA NNN NNN … -3'

Restriction site | Kozak sequence | Bases added for intein to be in frame for precise ligation | Target gene

Primer design (specific example Tpm3.1)

Beginning of Tpm3.1 gene:

Include start codon (ATG)

Top strand 5' ATG GAC GCC ATC AAG AAG AAG ATG→
Bottom strand 3' TAC CTG CGG TAG TTC TTC TTC TAC→

End of Tpm3.1 gene:

Do not include stop codon

←ACT TTA CTG GAG TTA AAC AAC ATG TAA 3' Top strand
←TGA AAT GAC CTC AAT TTG TTG TAC ATT 5' Bottom strand

Forward primer (option 1):

5' TT CGC GGC CGC GCC ACC ATG GAC GCC ATC AAG

NotI site | Kozak sequence | Tpm3.1 sequence

Reverse primer (option 1):

5' GGT TGC TCT TCC AAC CAT GTT GTT TAA CTC

SapI site | Tpm3.1 sequence

SapI digestion occurs 4 bases outside the recognition site. These bases are reintroduced to ensure in-frame ligation

Forward primer (option 2):

5' TTC GAA TTC GCC ACC ATG GAC GCC ATC AAG

EcoRI site | Kozak sequence | Tpm3.1 sequence

Reverse primer (option 2):

5' TT CAC TAG TGC ATC TCC CGT GAT GCA CAT GTT GTT TAA CTC

SpeI site | Tpm3.1 sequence

SpeI digestion removes 17 bases from intein that are reintroduced via the primer overhang during ligation

C

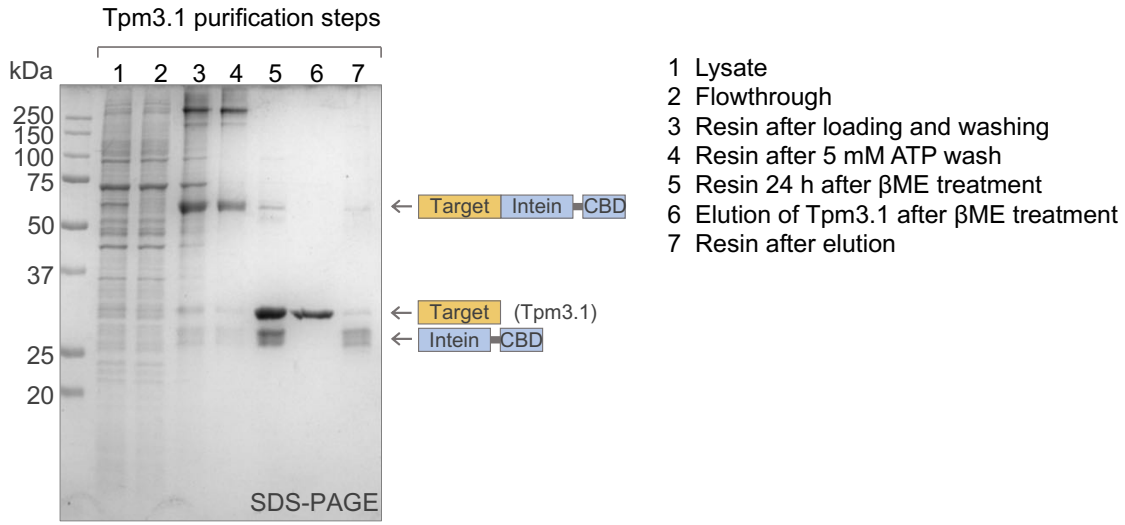

Figure S1. Instructions for cloning of a target gene into vector pJCX4. (A) Schematic representation of the expression cassette of vector pJCX4 for mammalian cell expression, including a restriction enzyme map of the multicloning site for the insertion of a target gene (see also Figure 1A). (B) Two examples of forward (5') and reverse (3') primer design to amplify a target gene for insertion into vector pJCX4, showing the general strategy (above) and a specific example for Tpm3.1 (below) (C) SDS-PAGE characterization and Coomassie Brilliant Blue R-250 (BIO-RAD) staining of the purification steps for Tpm3.1.

154 after self-cleavage of the intein (*Figure 1A, Figure S1A and B*). Growth and transfection of
155 Expi293F cells is carried out according to the manufacturer's protocol, with minor changes (see
156 Materials and methods). After harvesting and lysing cells, the fusion precursor protein is loaded
157 onto a chitin affinity resin. The high affinity of the CBD-chitin interaction allows for extensive
158 washing, and the resin can be analyzed during washing by SDS-PAGE to monitor the removal
159 of contaminants (*Figure 1B, Figure S1C*). The intein is then activated with the addition of a
160 reducing agent which allows the target protein to be released from the column.
161
162 We used this method here to express and purify the six most studied Tpm isoforms and α-
163 synuclein (*Figure 1C and D*). As an example, after extensive washing on the chitin resin, the
164 fusion protein Tpm3.1-intein-CBD is nearly contaminant free (step 1 in *Figure 1B*). Self-cleavage
165 of the intein, induced with β-mercaptoethanol for 24 h (step 2), is followed by elution of the
166 target protein (step 3). Although the proteins were mostly pure after the intein-affinity purification
167 step, most proteins here were additionally purified by ion exchange chromatography. Final
168 yields varied from protein to protein, ranging from 0.25 to 2 mg of purified proteins from 250 mL
169 of Expi293F culture.
170
171 **Post-translational modification of Expi293F-expressed Tpm and α-synuclein**
172
173 To evaluate the presence of PTMs and native N- and C-termini in the proteins expressed here
174 we used two approaches, tandem mass spectrometry (MS)-based proteomics and Pro-Q
175 Diamond phosphoprotein gel staining (Thermo Fisher Scientific). Fluorescent Pro-Q Diamond
176 staining is used to directly detect the presence of phosphate groups on tyrosine, serine, or
177 threonine residues in acrylamide gels. It is important to note that signaling cascades that get
178 activated during cell lysis can lead to increased dephosphorylation (67-69). Therefore,
179 phosphatase inhibitors can be used during cell lysis if necessary to preserve native
180 phosphorylation sites (70,71). We used this approach here in the Pro-Q Diamond staining
181 analysis (*Figure 2B and D*), but not for PTM proteomics analysis.
182
183 To ensure full peptide coverage during MS analysis, the expressed proteins were subjected to
184 digestions using three different enzymes: trypsin, chymotrypsin, and Glu-C. To establish the
185 identity of each peptide in the observed MS spectra, their masses were matched to the peptides
186 in a Tpm sequence database, using a false discovery rate (FDR) threshold of less than 1%
187 (*Table S1*). Full peptide coverage was obtained for all the proteins expressed, including Tpm
188 isoforms and α-synuclein, with one exception, Tpm4.2, for which coverage was 99% (*Figure 2A*
189 *and C, Figure S2*). This analysis revealed several interesting findings. All the proteins, including
190 α-synuclein, were Nt-acetylated, which as mentioned above is a precondition for optimal Tpm
191 polymerization along actin filaments (40,41). The three short Tpm isoforms analyzed (Tpm3.1,
192 Tpm3.2, Tpm4.2) were acetylated on the second residue. In other words, for these three
193 isoforms the initiator methionine is first removed during N-terminal processing and Nt-
194 acetylation then takes place on the second residue. Different N-terminal acetyl transferases
195 (NATs) likely acetylate Tpm isoforms at the initiator methionine and at position two. Based on
196 the known sequence specificity of the various human NATs (72), we anticipate isoforms
197 Tpm3.1, Tpm3.2, and Tpm4.2 with N-terminal sequence Met-Ala-Gly have their initiator
198 methionine removed by MetAP (methionine aminopeptidase) and then become acetylated by
199 NatA on Ala-2, whereas isoforms Tpm1.6, Tpm1.7, and Tpm2.1 with N-terminal sequence Met-
200 Asp-Ala are acetylated by NatB on the initiator methionine. α-Synuclein, with N-terminal
201 sequence Met-Asp-Val is also acetylated on the initiator methionine by NatB (73) (*Figure 2C*).
202 For all the proteins expressed here, intact and native C-termini peptides were identified (*Figure*
203 *2A and C, Figure S2*), confirming that self-cleavage of the intein proceeded as expected, without
204 the removal of any endogenous amino acids of the target protein or the presence of any extra

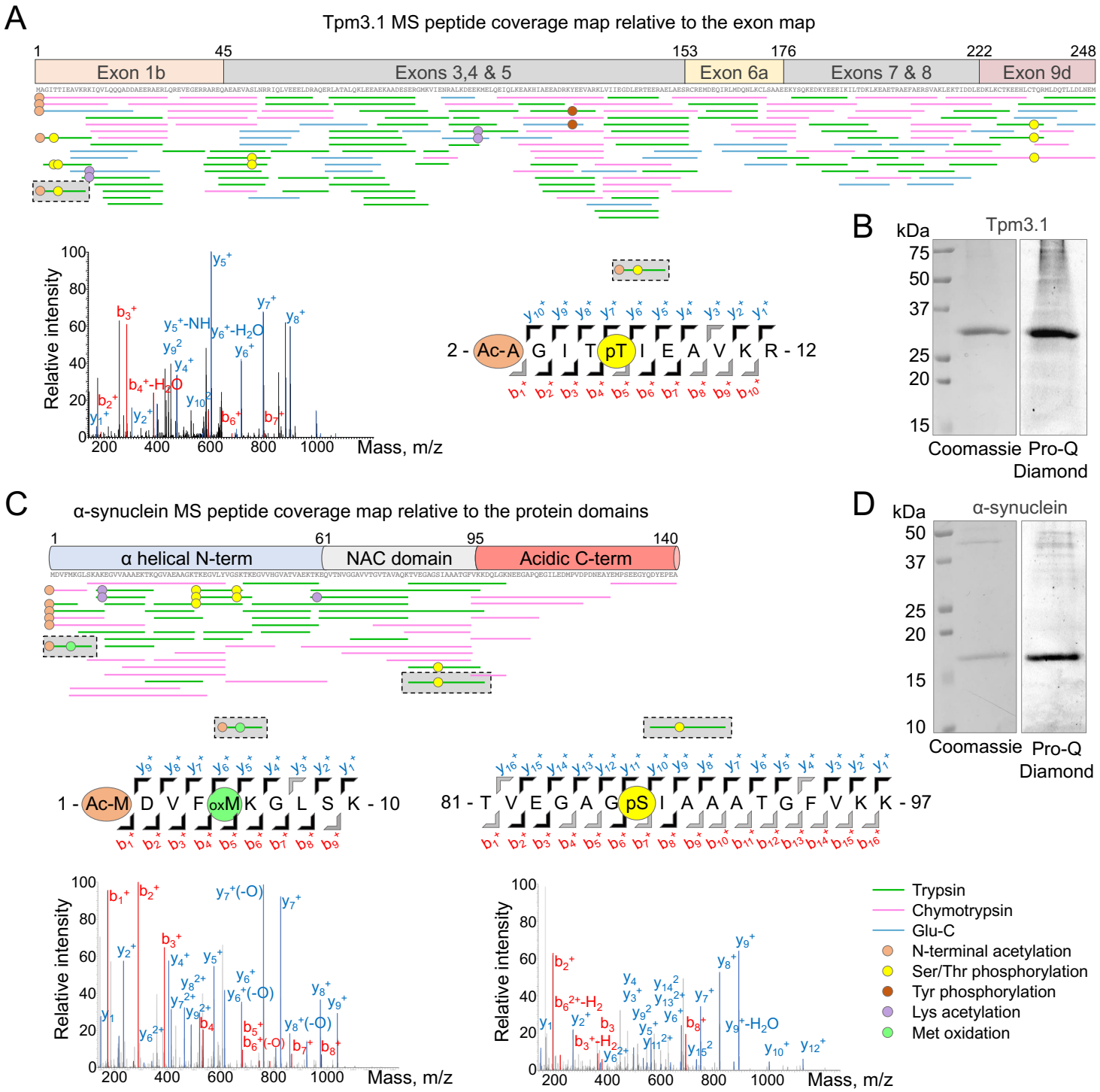

Figure 2. Post-translational modification analysis of Expi293F-expressed Tpm3.1 and α-synuclein. (A and C) Mass spectrometry peptide coverage maps of Tpm3.1 and α-synuclein, shown relative to exon and protein domain diagrams, respectively. Green, magenta and blue lines indicate peptides obtained by digestions with trypsin, chymotrypsin, and Glu-C, respectively, and whose masses were identified by mass spectrometry using a false discovery rate (FDR) threshold of < 1% (see also *Table S1* and *Figure S2*). Orange, yellow, red, purple, and green circles indicate Nt-acetylation, Ser/Thr phosphorylation, Tyr phosphorylation, Lys acetylation, and Met oxidation, respectively. The mass spectrometry spectra (MS2) of three representative peptides (highlighted by black dashed lines and gray background) are shown as examples, including N-terminal peptides of Tpm3.1 and α-synuclein, and a central peptide of α-synuclein. These peptides show different types of PTMs (Nt-acetylation, Ser/Thr phosphorylation, and Met oxidation). The MS2 spectra show the b (N-terminal) and y (C-terminal) fragment ions detected by mass spectrometry for each peptide. Sequence diagrams corresponding to the three spectra illustrate all the theoretical fragment ions colored black (observed experimentally) or gray (non-observed). (B and D) SDS-PAGE analysis of purified samples of Tpm3.1 and α-synuclein, using phosphatase inhibitors to reduce sample dephosphorylation during purification, and stained using either Coomassie Brilliant Blue R-250 (BIO-RAD) or Pro-Q Diamond Phosphoprotein Gel Stain (Thermo Fisher Scientific).

Table 1. PTMs identified in the human cell-expressed proteins (FDR < 1%)

Protein	Nt-acetylation	Ser/Thr phosphorylation	Tyr phosphorylation	Lys acetylation
Tpm1.6	Met-1	Ser-87, Ser-123, Ser-174, Thr-199, Ser-252		Lys-112, Lys-189
Tpm1.7	Met-1	Ser-87, Ser-174, Ser-245, Ser-252	Tyr-221	Lys-48
Tpm2.1	Met-1	Ser-87		Lys-48, Lys-77
Tpm3.1	Ala-2	Thr-5, Thr-6, Ser-51, Thr-234,	Tyr-126	Lys-13, Lys-104
Tpm3.2	Ala-2	Ser-51, Ser-155, Thr-216		Lys-169, Lys-190
Tpm4.2	Ala-2	Ser-6		Lys-169
α-synuclein	Met-1	Thr-33, Ser-42, Ser-87		Lys-12, Lys-60

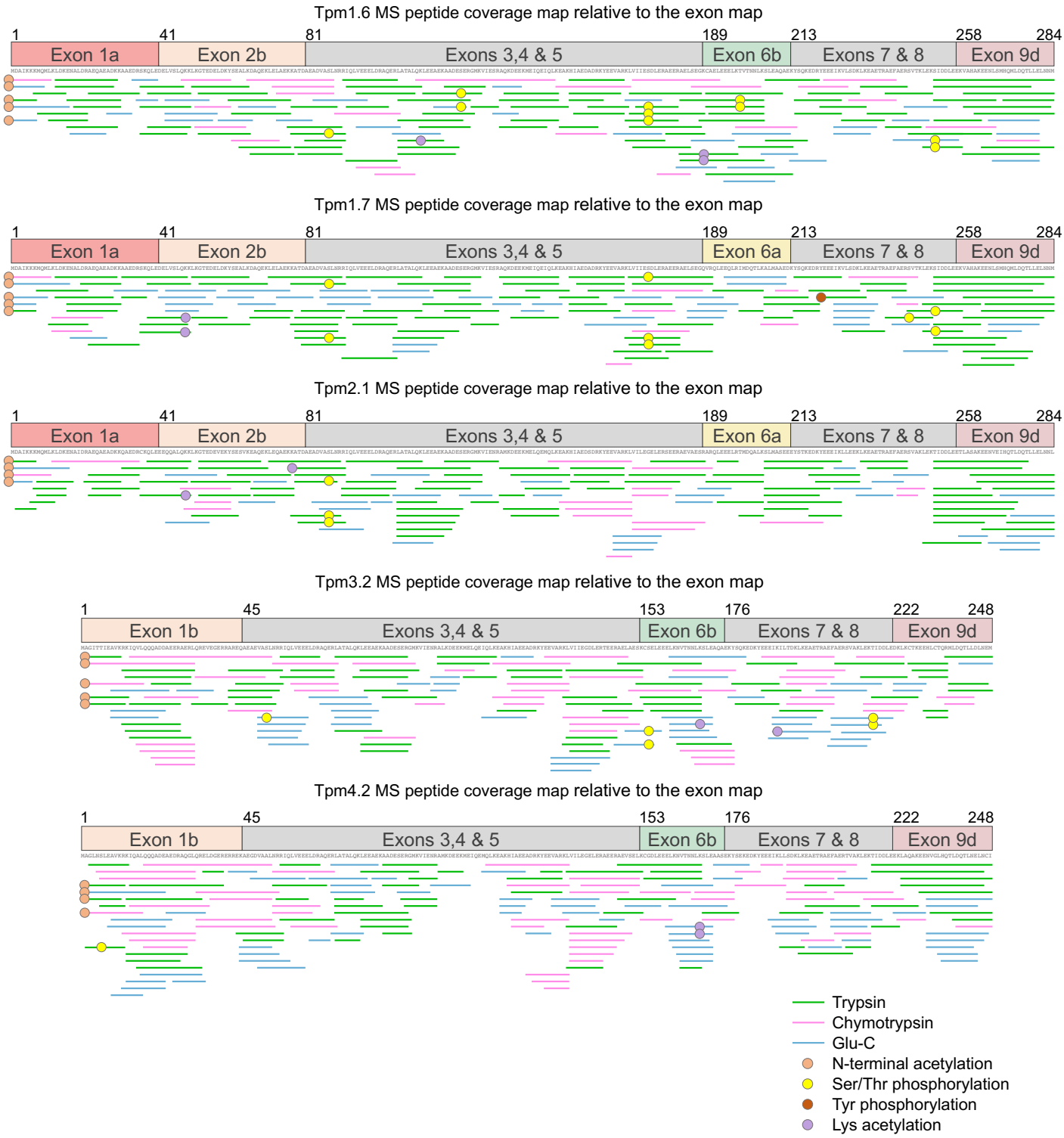

Figure S2. Post-translational modification analysis of Expi293F-expressed Tpm isoforms. Mass spectrometry peptide coverage maps of Tpm isoforms 1.6, 1.7, 2.1, 3.2, and 4.2, shown relative to the exon diagram of each isoform. Green, magenta and blue lines indicate peptides obtained by digestions with trypsin, chymotrypsin, and Glu-C, respectively, and whose masses were identified by mass spectrometry using a false discovery rate (FDR) threshold of less than 1% (see also Figure 2, Table S1, and Materials and methods). Orange, yellow, red, and purple circles indicate Nt-acetylation, Ser/Thr phosphorylation, Tyr phosphorylation, and Lys acetylation, respectively.

amino acids from the tag. Numerous phosphorylation sites, including serine/threonine and tyrosine phosphorylation, were identified in the expressed proteins with an FDR < 1% (*Table 1, Figure 2, Figure S2*). The identity of these phosphorylation sites is mostly consistent with previous phosphoproteomics studies curated by PhosphoSitePlus (74). Other forms of PTMs were also identified using the stringent FDR cutoff of < 1%, including most notably several sites of lysine acetylation (*Table 1, Figure 2, Figure S2, Table S1*). Methionine oxidation was also observed, including for instance α-synuclein Met-5 (*Figure 2C, Table S1*), however this is not a native modification but rather one that occurs during sample preparation for mass spectrometry (75). Table S1 contains a complete list of all the peptides and PTMs observed.

Comparison of the activities of Expi293F- vs. *E. coli*-expressed Tpm isoforms

The defining biochemical activity of Tpm is to decorate actin filaments, which by combinatorial association of different isoforms of both actin and Tpm can give rise to a large number of Tpm-actin copolymers with distinct properties and activities in cells (25). Accordingly, we used here actin cosedimentation assays to compare the actin-binding affinities of a representative group of three Expi293F-expressed Tpm isoforms, corresponding to three different genes and comprising both short (Tpm3.1) and long (Tpm1.6 and Tpm2.1) isoforms with differently processed N-termini (see Materials and methods). Quantification of multiple such experiments, using SDS-PAGE and densitometric analysis, and fitting of the data to a Hill equation revealed the parameters of the interactions of Tpm isoforms with F-actin, including the apparent dissociation constant (K_{app}) and Hill coefficient (a measure of the cooperativity of the interaction) (*Figure 3A, B and E, Figure S3*). This analysis confirmed binding of all three of the Tpm isoforms to F-actin, but with significantly higher affinity for Tpm1.6 (K_{app} = 0.32 ± 0.06 μM) than Tpm2.1 or Tpm3.1 (K_{app} = 1.78 ± 0.10 μM and 1.72 ± 0.09 μM, respectively). Interestingly, the latter two isoforms had very similar affinities for F-actin, despite one being one pseudo-repeat longer than the other and having differently processed N-termini.

We then compared the two most studied non-muscle isoforms (Tpm1.6 and Tpm3.1) with their *E. coli*-expressed counterparts, both with and without the addition at the N-terminus of three amino acids (Met-Ala-Ser) that have been widely used to mimic acetylation (41,76). This analysis revealed at least three interesting results. First, for the long isoform Tpm1.6, the Expi293F- and *E. coli*-expressed proteins had very similar affinities for F-actin when Met-Ala-Ser was added at the N-terminus (*Figure 3C and E*). However, the affinity of *E. coli*-expressed Tpm1.6 dropped ~15-fold when Met-Ala-Ser was not added. This result suggests that for Tpm1.6 the addition of Met-Ala-Ser adequately mimics N-terminal acetylation for binding to F-actin, although it remains to be shown whether this modification can fully account for other regulatory activities of Tpm1.6 in controlling the interactions of actin-binding proteins (ABPs) with the actin filament. Second, for the short isoform Tpm3.1 the two *E. coli*-expressed proteins, with and without Met-Ala-Ser at the N-terminus, had nearly identical affinities for F-actin, but lower than the affinity of Expi293F-expressed Tpm3.1 (*Figure 3D and E*). Therefore, for Tpm3.1 the addition of extra amino acids at the N-terminus cannot substitute for native Nt-acetylation, indicating that native PTMs added by Expi293F cells are necessary for function. We suspect this behavior may affect other Tpm isoforms, which is an important consideration since many studies have used extra N-terminal amino acids to substitute for Nt-acetylation irrespective of isoform. Third, it is known that most Tpm isoforms bind cooperatively to F-actin (77-79). Here, the isoforms that bound F-actin with lower affinity displayed higher cooperativity, and this was true among different isoforms as well as among variants of the same isoform expressed in different cell types. Thus, Tpm2.1 and Tpm3.1 exhibited higher cooperativity than Tpm1.6, whereas the *E. coli*-expressed Tpm isoforms that bound F-actin with lower affinity also showed higher cooperativity (*Figure 3E*).

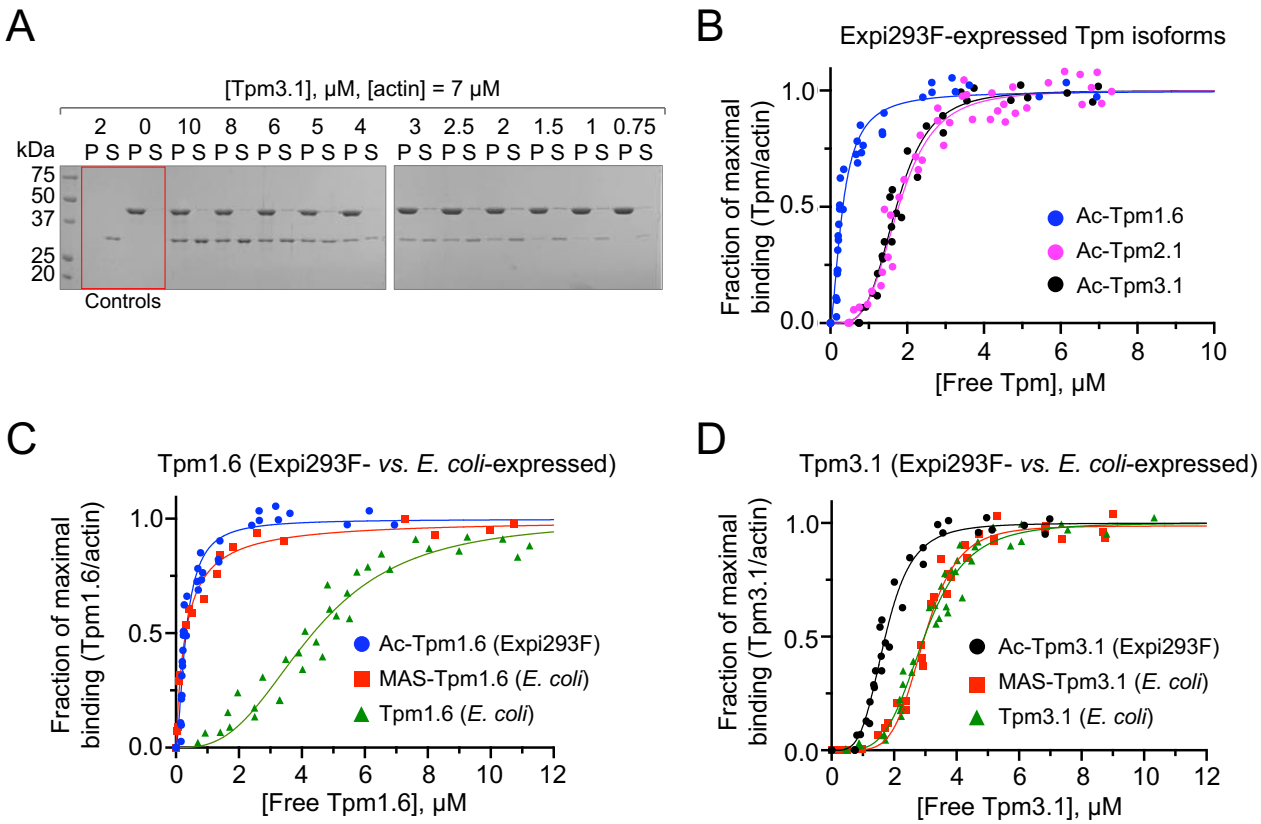

E

Tpm isoform	Expressed protein	Expression cell	K_{app} (μM)	Hill coefficient
Tpm1.6	Ac-Tpm1.6	Expi293F	0.32 ± 0.06	1.64 ± 0.45
	MAS-Tpm1.6	*E. coli*	0.31 ± 0.07	1.00 ± 0.21
	Tpm1.6	*E. coli*	4.34 ± 0.52	2.86 ± 0.78
Tpm3.1	Ac-Tpm3.1	Expi293F	1.72 ± 0.09	3.95 ± 0.78
	MAS-Tpm3.1	*E. coli*	2.97 ± 0.09	5.56 ± 0.96
	Tpm3.1	*E. coli*	2.97 ± 0.13	4.34 ± 0.59
Tpm2.1	Ac-Tpm2.1	Expi293F	1.78 ± 0.10	3.76 ± 0.74

Figure 3. Binding of Tpm isoforms to F-actin using cosedimentation analysis. (A) Representative SDS-PAGE cosedimentation analysis of Expi293F-expressed Tpm3.1 (0.75-10 μM) with F-actin (7 μM). Controls include actin alone, found mostly in the pellet fraction (P), and Tpm3.1 alone, found exclusively in the supernatant fraction (S). (B) Between three and four cosedimentation experiments were performed for each of the three Tpm isoforms analyzed (Tpm1.6, Tpm2.1, Tpm3.1; color-coded), the density of the bands in the gels were quantified and data were plotted as the fraction of maximal binding *vs*. the free concentration of each Tpm isoform (see *Figure S3* and Materials and methods). The data were fit to a Hill equation to obtain the dissociation constant (K_{app}) and Hill coefficient of each interaction. (C and D) experiments similar to those shown in panels *A* and *B* were performed to compare the F-actin-binding affinities of Expi293F-expressed Tpm1.6 and Tpm3.1 with their *E. coli*-expressed counterparts, with and without the N-terminal addition of Met-Ala-Ser (MAS), a modification thought to mimic acetylation {Gateva, 2017 #12568;Palm, 2003 #12954}. (E) Parameters of the fits shown in panels B to D, including K_{app} and Hill coefficient.

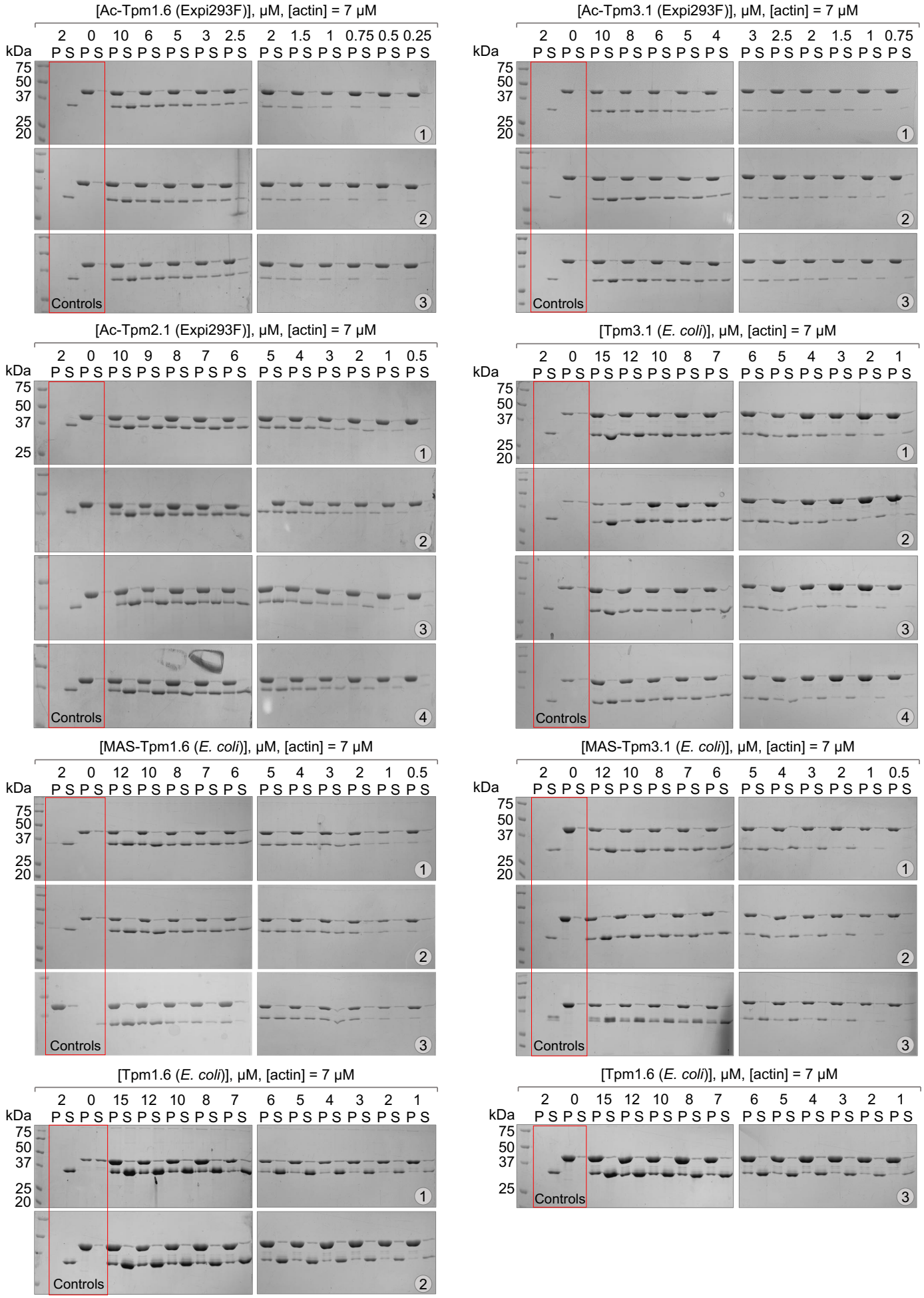

Figure S3. Cosedimentation of Tpm isoforms with F-actin**.** Cosedimentation analysis of the interactions of Tpm isoforms with F-actin using 12% SDS-PAGE gels, showing Expi293F-expressed Tpm1.6, Tpm2.1, and Tpm3.1 and *E. coli*-expressed Tpm1.6 and Tpm3.1 with and without the addition of Met-Ala-Ser (MAS) at the N-terminus to mimic Nt-acetylation. The actin concentration in all the experiments was 7 μM, whereas the concentration of Tpm varied for each experiment and is shown on the top of the gels. Controls include actin alone, found mostly in the pellet fraction (P), and Tpm alone, found exclusively in the supernatant fraction (S) for all the proteins analyzed. This data was used to produce the plots and data fits shown in Figure 3.

256
257 **Non-muscle Tpm isoforms can form heterodimers**
258
259 The actin filaments of the contractile apparatus of muscle cells are decorated with two or more
260 Tpm isoforms, which often associate as heterodimers (80-83). For instance, in skeletal muscle
261 Tpm1.1/Tpm2.2 (also known as isoforms α and β) heterodimers form more favorably than
262 Tpm1.1/Tpm1.1 homodimers (81). It is unknown whether non-muscle Tpm isoforms can also
263 form heterodimers in cells.
264
265 To explore this question, we modified the mammalian cell expression system described here to
266 coexpress pairs of Tpm isoforms. We designed a new mammalian cell expression vector,
267 containing an internal ribosomal entry site (IRES) inserted in between two multi-cloning sites
268 (MCS), one for each Tpm isoform being coexpressed (*Figure 4A*). The use of the coexpression
269 IRES vector, instead of cotransfection with two separate vectors, ensures that similar amounts
270 of the two Tpm isoforms are expressed together in time and space. Adjacent to MCS1 and
271 MCS2 the vector contains a V5 and a FLAG affinity tag, respectively. In this way, the
272 coexpressed Tpm isoforms have native N-termini, but either V5 or FLAG affinity tags added at
273 the C-terminus. These tags are used for tandem affinity purification and detection via Western
274 blot analysis (*Figure 4B*), a method we previously used to study wild-type/mutant heterodimers
275 of IRSp53 (84). The presence of these tags likely disrupts the head-to-tail interaction of Tpm
276 coiled coils along F-actin, but because coiled coil formation does not depend on Tpm's ability to
277 bind F-actin, these tags were not removed for the experiments described here. When two Tpm
278 isoforms are coexpressed using this strategy, they can form either two independent
279 homodimers, heterodimers or a combination of homodimers and heterodimers. To discriminate
280 among these possibilities, we purify the mixture on a FLAG resin, wash extensively, and the
281 eluted sample is then analyzed by anti-FLAG and anti-V5 Western blotting (*Figure 4B*). The
282 presence of an anti-V5 signal in the eluted sample (but not in the last wash) is a strong
283 indication of heterodimer formation. This procedure is illustrated here for the coexpressed
284 isoform pair Tpm3.1-V5/Tpm4.2-FLAG (*Figure 4C*). Note that the anti-FLAG and anti-V5 signals
285 disappear almost entirely in the last wash, but both signals show up strongly in the eluted
286 sample, indicating that any Tpm3.1-V5 that was retained in the FLAG resin was forming
287 heterodimers with Tpm4.2-FLAG.
288
289 Because heterodimerization of long muscle isoforms has been demonstrated (80,81,85), the
290 analysis here focused on four short, non-muscle Tpm isoforms: Tpm3.1, Tpm3.2, Tpm3.5, and
291 Tpm4.2. Note that Tpm isoforms of different lengths are unlikely to heterodimerize since this
292 would lead to parts of the hydrophobic core of the coiled coil being exposed to the solvent. We
293 co-expressed the following pairs: Tpm3.1-V5/Tpm3.2-FLAG, Tpm3.1-V5/Tpm4.2-FLAG, and
294 Tpm3.5-V5/Tpm4.2-FLAG, which all formed heterodimers (*Figure 4D*). To control for potential
295 differences in the expression levels of the proteins cloned into MCS1 and MCS2, we switched
296 the order of isoforms and coexpressed the pair Tpm3.2-V5/Tpm3.1-FLAG, which also formed a
297 heterodimer. Another control showed that V5- and FLAG-tagged isoforms Tpm3.1 and Tpm3.2
298 form homodimers despite the different tags. Finally, Tpm3.1-FLAG cloned alone into MCS2
299 (MCS1 empty) also eluted as a homodimer and no anti-V5 signal was detected in the eluted
300 sample (*Figure 4D*).
301
302 These results strongly suggest that Tpm3.1, Tpm3.2, Tpm3.5, and Tpm4.2, and likely other non-
303 muscle isoforms can form heterodimers as well as homodimers in cells when coexpressed
304 together. We then asked whether they would preferentially reassociate as homodimers or
305 heterodimers after boiling *in vitro*, which unfolds the coiled coil, as shown for muscle isoforms
306 (86-88). For this, we modified the procedure described above introducing two additional steps;

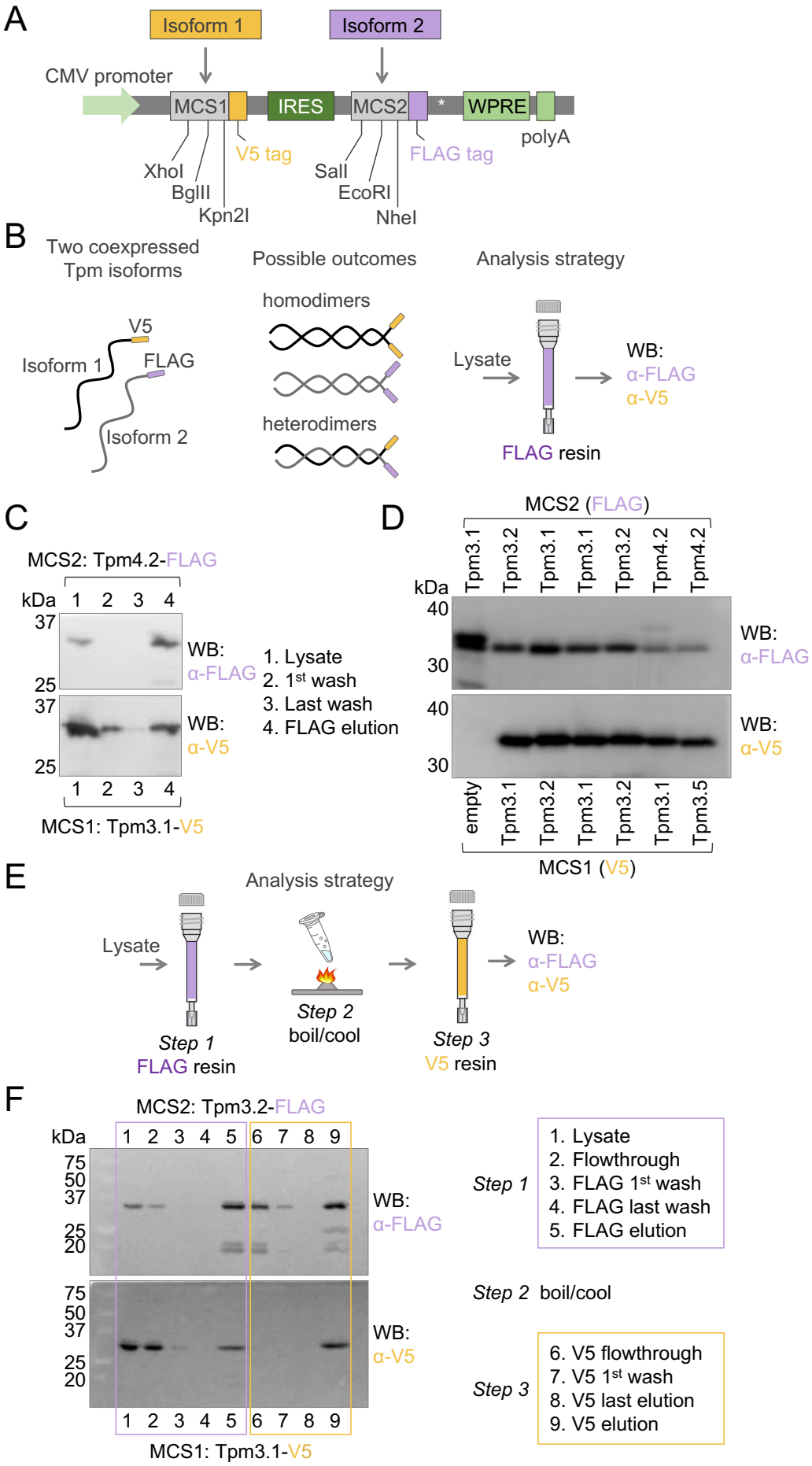

Figure 4. Heterodimerization of non-muscle Tpm isoforms. (A) Schematic representation of the MCS1-IRES-MCS2 elements of vector pJC8 used for coexpression of pairs of Tpm isoforms, including a depiction of the restriction sites and affinity tags (FLAG and V5) associated with each MCS. (B) Illustration of the potential association of coexpressed Tpm pairs as homodimers or heterodimers and strategy for the FLAG tag-based purification and Western blot-based detection of such species using anti-FLAG and anti-V5 antibodies. (C) Illustration of this strategy for the coexpressed pair of Tpm3.1-V5 and Tpm4.2-FLAG, showing the presence of both isoforms, i.e. heterodimers reactive to both anti-FLAG and anti-V5 antibodies, in the elution sample after extensive washing on the FLAG resin. (D) Western blot analysis of the FLAG elution samples from seven such experiments, including six Tpm pairs and a control experiment with Tpm3.1-FLAG cloned into MCS2 and no Tpm isoform cloned into MCS1. (E) Experimental design for the detection of Tpm heterodimers after unfolding and refolding. Following the FLAG elution, samples are boiled and cooled and then purified on a V5 resin. (F) Illustration of this strategy for the coexpressed pair of Tpm3.1-V5 and Tpm3.2-FLAG. After extensive washing, the Western blot detection of anti-FLAG and anti-V5 signals in the sample from the V5 resin demonstrates that Tpm3.1/Tpm3.2 heterodimers formed spontaneously during refolding.

307 after purification on the FLAG resin, the eluted samples were boiled, then allowed to slowly
308 refold during cooling, repurified on a V5 resin, and then analyzed by anti-FLAG and anti-V5
309 Western blotting (*Figure 4E*). We analyzed in this manner the pair Tpm3.1-V5/Tpm3.2-FLAG
310 and monitored each step of this procedure by Western blotting (*Figure 4F*). The initial steps of
311 the procedure (i.e. purification on the FLAG resin) confirmed the formation of heterodimers, as
312 described above (*Figure 4D*). After boiling/cooling the sample was loaded onto the V5 resin.
313 The flowthrough from the V5 resin reacted only with the anti-FLAG antibody, indicating that
314 some of the heterodimers had reassociated as homodimers. Yet, the V5 elution showed strong
315 anti-FLAG and anti-V5 signals. Any Tpm3.2-FLAG retained in the V5 resin was likely forming
316 heterodimers with Tpm3.1-V5. Together, the data presented here show that non-muscle Tpm
317 isoforms can form both homodimer and heterodimers in cells and *in vitro*.
318
319 **Discussion**
320
321 **Main features and general applicability of the expression-purification method**
322
323 We have developed a novel method for protein expression and purification that integrates the
324 advantages of mammalian cell expression with those of an intein-CBD purification tag. The
325 mammalian cells used, Expi293F, grow to high density in suspension and are adapted for high-
326 yield protein expression. More importantly, these cells naturally contain the necessary folding
327 and PTM machineries to produce fully native human proteins. The intein-CBD tag, on the other
328 hand, provides three key advantages. First, it is a high-affinity tag that allows for extensive on-
329 column washing, such that high protein purity can be achieved in a single purification step.
330 Second, this is a self-cleavable tag, which can be activated on-column, bypassing the necessity
331 for enzymatic cleavage after purification and additional purification associated with other tags
332 that can in some cases produce non-specific cleavage and introduces two new contaminants,
333 i.e. the cleavage enzyme and the released affinity tag. Third, through proper design of the
334 cloning primers (as shown in *Figure S1*) self-cleavage of the intein can take place precisely after
335 the last C-terminal amino acid of the expressed protein, without the deletion of endogenous
336 amino acids or the presence of extra amino acids from the tag. One potential drawback of this
337 system is that a certain amount of premature cleavage may take place in the reducing
338 environment of the cytoplasm of Expi293F cells, which ultimately reduces protein yields. Yet, for
339 all the proteins expressed here yields of ~1 mg of highly pure proteins were obtained from
340 relatively small Expi293F cultures of 250 mL. Such protein amounts are clearly sufficient for
341 most biochemical and structural studies and the technology is cost permissive for most
342 laboratories possessing a mammalian cell incubator. The combined benefits and relative
343 simplicity of this method make it easily adaptable for the expression of most human proteins,
344 and particularly those whose activities depend upon key PTMs. Thus, while the initial motivation
345 for this work was the expression of several cytoskeletal proteins of interest to our laboratory,
346 such as Tpm, we extended it here to the expression of α-synuclein, a protein of intensive
347 interest and a notable target of many PTMs (52,53). To facilitate the adoption of this system, we
348 are depositing the two vectors developed here with the Addgene plasmid repository
349 (www.addgene.org).
350
351 **PTMs of human cell-expressed non-muscle Tpm isoforms**
352
353 The use of the human cell-expression system described here allowed us to make several
354 discoveries. One of these discoveries concerns the presence of numerous forms of PTMs,
355 including Nt-acetylation, Ser/Thr and Tyr phosphorylation and Lys acetylation in non-muscle
356 Tpm isoforms (*Figure 2A*, *Figure S2*, *Table 1*). We have limited the list of PTMs reported here to
357 sites detected with very high fidelity (FDR < 1%), but many other sites were detected with

358 relatively high confidence (FDR < 5%) and could possibly play functional roles (*Table S1*). The
359 importance of Ser/Thr phosphorylation in muscle Tpm isoforms has been recognized since the
360 seventies (89,90), and a more recent study suggests that phosphorylation of Ser-283 near the
361 C-terminus of striated muscle Tpm (Tpm1.1) enhances the stiffness of the head-to-tail
362 interaction (43) . Virtually nothing, however, is known about the role of Ser/Thr phosphorylation
363 in non-muscle Tpm isoforms. Curiously, among the phosphorylation sites observed here,
364 several occur near the N- and/or C-terminal ends of Tpm3.1, Tpm1.6, Tpm1.7, Tpm3.2, and
365 Tpm4.2, and could possibly have a similar role as in muscle Tpm1.1, by modulating the stiffness
366 of the head-to-tail interaction. To our knowledge, the role Tyr phosphorylation in Tpm isoforms
367 remains unexplored, and our finding here of Tyr phosphorylation sites in Tpm3.1 and Tpm1.7
368 opens an interesting new line of inquire to understand the role of this modification. Lys
369 acetylation of Tpm isoforms is also virtually unexplored. One of the Lys acetylation sites
370 detected here occurs near the N-terminus of Tpm3.1 and could also modulate the
371 polymerizability of this isoform along actin filaments, as *in vitro* studies have suggested for
372 muscle Tpm (91). A recent study also finds that Lys acetylation of F-actin decreases Tpm-
373 dependent inhibition of actomyosin activity (92). Lys acetylation of non-muscle Tpm isoforms
374 could have a similar effect, by modulating the interactions of ABPs. The presence and extent of
375 Nt-acetylation among non-muscle Tpm isoforms is to this day questioned (93). Since ~90% of
376 human proteins are Nt-acetylated (58) and Nt-acetylation plays a crucial role in the
377 polymerization of muscle Tpm isoforms (41), it is not surprising that we found here that all the
378 non-muscle isoforms analyzed were Nt-acetylated. What is more, we did not detect a single N-
379 terminal peptide that was not acetylated, suggesting that N-terminal acetylation is a constitutive
380 modification for all Tpm isoforms. More surprising, but consistent with the known sequence
381 specificity of human NATs (72), was the observation that the short Tpm isoforms (Tpm3.1,
382 Tpm3.2, Tpm4.2) undergo Nt-acetylation on the second residue, after removal of the initiator
383 Met by MetAP, which the PTM machinery of Expi293F cells was also able to achieve for these
384 overexpressed proteins. These three isoforms are likely Nt-acetylated by NatA, whereas the
385 long isoforms (Tpm1.6, Tpm1.7, Tpm2.1) are likely Nt-acetylated by NatB on the initiator Met
386 (72).
387
388 **Different activities of Tpm isoforms expressed in human and *E. coli* cells**
389
390 The vast majority of *in vitro* studies on Tpm isoforms have used *E. coli*-expressed proteins. For
391 years, these studies have used the addition of extra amino acids at the N-terminus of Tpm as a
392 way to mimic Nt-acetylation (40,41,48,49) and have assumed that this modification fully
393 replicates the natural capacity of Tpm to polymerize along actin filaments. By comparing for the
394 first time side-by-side the F-actin-binding activity of naturally acetylated and *E. coli*-expressed
395 Tpm isoforms ± Nt-acetylation-mimics we have shown here that this assumption is not always
396 true. Thus, while the N-terminal addition of Met-Ala-Ser mostly restores the F-actin-binding
397 affinity of *E. coli*-expressed Tpm1.6, it fails to do the same for Tpm3.1 (*Figure 3*). Tpm3.1 is a
398 short isoform, whereas Tpm1.6 is a long isoform and interacts with one more actin protomer
399 along F-actin. While this difference could possibly explain their different behaviors in these
400 experiments, it appears prudent to test this effect individually for each Tpm isoform, particularly
401 that this work provides a solution to the problem of Nt-acetylation. Indeed, Tpm2.1 is also a long
402 isoform, but we found its affinity for F-actin to be very similar to that of Tpm3.1 (*Figure 3A*). We
403 also noticed an interesting correlation between affinity and cooperativity; lower Tpm binding
404 affinity for F-actin correlates with higher cooperativity of the interaction, both among naturally
405 occurring isoforms or within a single isoform with different head-to-tail interaction sequences
406 (*Figure 3E*). Although we could not find a previous reference to this correlation, it is intuitively
407 clear that as the affinity of single Tpm dimers for F-actin becomes lower, binding to F-actin
408 would become increasingly dependent on the pre-polymerization of Tpm into mini-filaments of

409 ever-growing length through head-to-tail interaction. This is also why a strong head-to-tail
410 interaction, which Nt-acetylation favors, enhances binding to F-actin.
411
412 **Non-muscle Tpm isoforms can form heterodimers *in vitro* and in cells**
413
414 It has long been known that muscle Tpm isoforms function as a mixture of homodimers and
415 heterodimers (81). Similarly, we have shown here that non-muscle Tpm isoforms purify from
416 cells as both homodimers and heterodimers, and that their ability to heterodimerize is retained
417 after boiling and cooling *in vitro*, with no apparent preference for one form of association vs.
418 another. This is an important finding, since Tpm heterodimerization can further expand the
419 range and functional diversity of Tpm-actin copolymers with segregated localization and function
420 in cells. The prevalence of heterodimers in cells could be dictated by the time, location and
421 amount of expression of one isoform vs. another.
422
423 In summary, we have developed a novel method for the expression of fully native proteins in
424 human cells, we have demonstrated its applicability to two types of proteins of general interest,
425 we have used this method to make new discoveries about non-muscle Tpm that had so far
426 resisted investigation, and we have provided the scientific community access to our newly-
427 developed vectors to facilitate the adoption of this method.
428
429
430 **Materials and methods**
431
432 **Human cell expression vectors**
433
434 *Vector pJCX4*: The QuickChange site-directed mutagenesis kit (Agilent Technologies, Santa
435 Clara, CA) was used to remove two SapI restriction sites from vector pEGFP-C1 (Takara Bio
436 USA, Mountain View, CA). A Woodchuck hepatitis virus (WHP) posttranscriptional regulatory
437 element (WPRE) was added between the XbaI and MfeI sites of the multi-cloning site (MCS).
438 The MCS-intein-chitin binding domain of vector pTXB1 (New England Biolabs, Ipswitch, MA)
439 was then inserted between sites NheI and Kpn2I, and the MCS of vector pEGFP-C1 was
440 removed by annealed oligos which were ligated between sites Kpn2I and XbaI. The vector is
441 depicted in figure 1*A*.
442
443 *Vector pJC8*: The intein-CBD cassette was removed from vector pJCX4 and replaced with an
444 internal ribosome entry site (IRES) element between sites BamHI and BspE1. Two new
445 multicloning sites, one containing a V5- and the other a FLAG-affinity tag, were introduced on
446 either side of the IRES using annealing oligos. The V5 and FLAG epitope tags provide clear
447 signals by Western blot analysis and are used here to recognize the expressed Tpm isoforms.
448 The MCSs and IRES region of the vector are depicted in figure 4*A*.
449
450 **Cloning of Tpm isoforms and α-synuclein**
451
452 The following cDNAs were used in cloning (NCBI codes): Tpm1.6 (NM_001018004), Tpm1.7
453 (NM_001018006), Tpm2.1 (NM_213674), Tpm3.1 (NM_153649), Tpm3.2 (NM_001043351),
454 Tpm4.2 (NM_003290), α-synuclein (NM_000345.4). The cDNAs were cloned into vector pJCX4
455 by PCR-amplification with primers that included the NotI (5') and SapI (3') restriction enzyme
456 sites (*Figure 1, Figure S1*). The genes encoding isoforms Tpm1.6 and Tpm3.1 with added N-
457 terminal Met-Ala-Ser in vector pBAT4 were a gift from Dr. Pekka Lappalainen. The two isoforms
458 were also cloned without N-terminal extensions into vector pBAT4 by PCR-amplification with
459 primers that included the NcoI (5') and either BamHI or XhoI (3') restriction enzyme sites. Four

460 of the Tpm isoforms (Tpm3.1, Tpm3.2, Tpm3.5, Tpm4.2) were separately cloned as pairs into
461 the IRES-containing vector pJC8 (see above) using PCR primers which included XhoI and
462 BspEI (MCS1) or NotI and NheI (MCS2) on their overhangs. For this, the cDNA encoding
463 isoform Tpm3.5 was generated starting from Tpm3.1 (amino acids 1-222) and the nucleotides
464 encoding for the C-terminal 26 amino acids that differ among these two isoforms were added by
465 overlap extension PCR. All the primers used in this study are listed in Table S2.
466
467 **Protein expression in Expi293F cells and intein-based purification**
468
469 Expression was carried out with minor changes to the manufacture's protocol for the Expi293
470 Expression System Kit (Thermo Fisher Scientific, Waltham, MA). Expi293F cells were grown in
471 Expi293 media to a density of 2.5 x 10^6 cells/mL. Cultures were incubated on an orbital shaker
472 (125 rpm) at 37°C using an Isotemp incubator (Thermo Fisher Scientific, Waltham, MA) with a
473 humidified atmosphere of 8% CO_2. Pure plasmid DNA (1 µg per mL of Expi293F culture) and
474 polyethylenimine (PEI, 3 µL per mL of Expi293F culture) were added to separate 5 mL aliquots
475 of 37°C Opti-MEM (Thermo Fisher Scientific), mixed after 5 min, and incubated for 30 min at
476 25°C and then added to the Expi293F cell culture. Cultures were grown for 48-72 h, optimized
477 for each protein. Cells were harvested by centrifugation (4,000 x g) at 4°C for 10 min.
478
479 For purification, cell pellets were resuspended in 20-35 mL of lysis buffer (20 mM HEPES pH
480 7.5, 500 mM NaCl, 1 mM DTT). Cells were lysed using a Dounce glass piston homogenizer
481 (Kontes Glass, Vineland, NJ) and the supernatants were clarified by centrifugation at 48,000 x g
482 at 4°C for 20 min. The clarified supernatants were loaded onto 15 mL chitin resin (packed into a
483 column) pre-equilibrated with lysis buffer and washed extensively. Self-cleavage of the intein
484 was activated with the addition of 50 mM β-mercaptoethanol at 25°C for 24 h. The expressed
485 proteins were then eluted with lysis buffer, dialyzed overnight into A-buffer (20 mM HEPES pH
486 7.5, 50 mM NaCl) and further purified on a Source Q column (MilliporeSigma, St. Louis, MO)
487 using a 50-300 mM NaCl gradient. Peak fractions were dialyzed into storage buffer (20 mM
488 HEPES pH 7.5, 50 mM NaCl), flash frozen in liquid nitrogen and stored at -80°C.
489
490 ***E. coli* expression and purification of Tpm isoforms**
491
492 Tpm isoforms Tpm1.6 and Tpm3.1 (with and without Met-Ala-Ser at the N-terminus) were
493 expressed in ArcticExpress(DE3) RIL cells (Agilent Technologies), grown in Terrific Broth (TB)
494 medium for 6 h at 37°C to an optical density of ~1.5-2 at 600 nm (OD_{600}), followed by 24 h at
495 10°C in with 0.4 mM isopropyl-β-D-thiogalactoside (IPTG). Cells were harvested by
496 centrifugation (4,000 x g) and resuspended in 20 mM HEPES (pH 7.5), 100 mM NaCl, 1 mM
497 EDTA, and 1 mM phenylmethanesulfonyl fluoride (PMSF). Cells were boiled in a water bath for
498 10 min, cooled on ice for 10 min, and clarified by centrifugation at 48,000 x g for 20 min at 4°C.
499 Sodium acetate (1 M, pH 4.5) was added to the clarified supernatant containing the Tpm
500 isoforms (that are heat-stable) until the solution reached the isoelectric point for precipitation of
501 each isoform (4.5-4.7). The solutions were then centrifuged at 48,000 x g to pellet the Tpm
502 isoforms. Pellets were dissolved in A-buffer (20 mM HEPES pH 7.5, 100 mM NaCl) and
503 dialyzed in the same buffer overnight. Proteins were loaded on Source Q ion exchange
504 (MilliporeSigma) and eluted with a 100-500 mM NaCl gradient. Peak fractions containing pure
505 proteins were dialyzed in storage buffer (20 mM HEPES pH 7.5, 50 mM NaCl), flash frozen in
506 liquid nitrogen and stored at -80°C.
507
508 **Preparation of samples for proteomics analysis**
509

510 Gel bands of the purified proteins were cut and destained with 100 mM ammonium
511 bicarbonate/acetonitrile (50:50). The bands were reduced in 10 mM dithiothreitol and 100 mM
512 ammonium bicarbonate for 60 min at 52°C. The bands were then alkylated with 50 mM
513 iodoacetamide and 100 mM ammonium bicarbonate at 25°C for 1 h in the dark. The proteins
514 were digested with enzymes (trypsin, chymotrypsin, or Glu-C) at 37°C for 12 h. Supernatants
515 were removed and transferred to fresh tubes. Additional peptides were extracted from the gel by
516 adding 50% acetonitrile and 1% TFA and shaking for 10 min. The supernatants were combined
517 and dried. The dried samples were reconstituted in 0.1% formic acid for mass spectrometry
518 analysis.
519
520 **Proteomics analysis by nano-LC-MS/MS**
521
522 Peptides were analyzed on a Q-Exactive Orbitrap Mass Spectrometer attached to an Easy-nLC
523 (Thermo Fisher Scientific) at 400 nL/min. Peptides were eluted with a 25 min gradient of 5-32%
524 ACN followed by 5 min 90% ACN and 0.1% formic acid. The data-dependent acquisition mode
525 with a dynamic exclusion of 45 sec was used for analysis. A full MS scan range of 350-1200 m/z
526 was collected, with a resolution of 70 K, maximum injection time of 50 ms, and automatic gain
527 control (AGC) of $1x10^6$. A series of MS2 scans were then acquired for the top 12 most abundant
528 ions of the MS1 scans. Ions were filtered with charge 2–4. An isolation window of 2 m/z was
529 used with the quadruple isolation mode. Ions were fragmented using higher-energy collisional
530 dissociation (HCD), with a collision energy of 27%. Orbitrap detection was used with a scan
531 range of 140-2000 m/z, resolution of 30 K, maximum injection time of 54 ms and AGC of
532 50,000. All the samples were analyzed using a multiplexed parallel reaction monitoring (PRM)
533 method based on a scheduled inclusion list containing the target precursor ions. Full MS scans
534 were acquired on the Orbitrap from 350–1200 m/z at a resolution of 60,000, using an AGC of
535 50,000. The minimum threshold was set to 100,000 ion counts. Precursor ions were fragmented
536 with the quadrupole using an isolation width of 2 m/z units, a maximum injection time of 50 ms
537 and AGC of 10,000.
538
539 **Proteomics MS Data Analysis Including Peptide Identification and Quantification**
540
541 The mass spectrometry raw spectra were processed using Proteome Discoverer version 2.3
542 (Thermo Fisher Scientific). The spectra were searched against a database of target protein
543 sequences using default setting: precursor mass tolerance of 10 ppm, fragment mass tolerance
544 of 0.02 Da, enzymes specific cleavage sites, and up to two missed cleavages. Cysteine
545 carbamidomethylation was set as a fixed modification, while methionine oxidation and N-
546 terminal or lysine acetylation were set as variable modifications. The search results were filtered
547 using the target-decoy approach with the false discovery rate (FRD) cutoff of < 1% at the
548 peptide and protein levels. To identify PTMs, the raw data were re-processed with the program
549 MetaMorepheus version 0.0.316 optimized for PTM analysis (94). The calibrate, G-PTM-D, and
550 search tasks of the program were used with default parameters, including default fixed and
551 variable modifications, precursor mass tolerance of 5 ppm, enzyme specific cleavage, up to two
552 missed cleavages, and an FRD cutoff of < 1% at the peptide and protein levels.
553
554 **Cosedimentation assays**
555
556 Actin filaments at a fixed concentration of 7 μM were incubated for 30 min at 25°C with
557 increasing Tpm concentrations in cosedimentation buffer (20 mM HEPES pH 7.5, 200 mM
558 NaCl, 5 mM $MgCl_2$) and a total volume of 100 μL. The reactions were centrifuged for 30 min at
559 80,000 rpm (280,000 rcf) to pellet F-actin and any bound Tpm (*Figure 3A, Figure S3*). For each
560 Tpm protein, the cosedimentation experiments were repeated three or four times (*Figure S3*).

561 After centrifugation, 100 µL of the supernatants were mixed with 25 µL of 4x Laemmli SDS-
562 PAGE loading buffer (S fraction). Pellets were gently washed with 100 µL of cosedimentation
563 buffer, to remove any remaining soluble protein, and resuspended in 100 µL of cosedimentation
564 buffer and mixed with 25 µL of 4x Laemmli SDS-PAGE loading buffer (P fraction). Identical
565 volumes (7 µL) of the P and S fractions were analyzed on SDS-PAGE gels, Coomassie-stained,
566 and the bands were densitometrically quantified with the program Image Lab (BIO-RAD). In the
567 absence of actin filaments, all the Tpm isoforms were found in the S fraction, whereas most of
568 the actin was found in the P fraction with or without Tpm (*Figure 3A, Figure S3*). In the presence
569 of actin filaments, Tpm cosedimented with actin to different degrees. The free Tpm
570 concentration (plotted on the x-axis) was determined by dividing the intensity of the Tpm band in
571 the S fraction by the sum of the intensities of the Tpm bands in the S and P fractions and
572 multiplied by the total Tpm concentration. The fraction of Tpm bound in the pellet was
573 determined by dividing the intensities of the Tpm and actin bands in the pellet fraction.
574 According to a commonly used convention (95,96), we plotted on the y-axis the fraction of
575 maximal Tpm binding to F-actin, determined by normalizing the ratio of the intensities of the
576 Tpm and actin bands in the pellet fraction to the plateau value for each Tpm sample (i.e. the
577 maximum fraction of Tpm/actin in the pellet fraction). This allows to compare side-by-side Tpm
578 isoforms with different F-actin-binding affinities by plotting the fraction of maximal binding vs. the
579 free Tpm concentration and fitting the data to a Hill equation for cooperative binding. We used
580 the program Prism 9.0.0 (GraphPad) for fitting with a "specific binding with Hill slope" model,
581 which yielded the apparent dissociation constant (K_{app}) and Hill coefficient for each interaction
582 (*Figure 3E*).
583
584 **Detection of non-muscle Tpm heterodimers**
585
586 Expi293F cell cultures (25 mL) expressing pairs of Tpm isoforms using the IRES-containing
587 vector pJC8 (see above) were resuspended in FLAG lysis buffer (phosphate buffered saline, 1
588 mM EDTA, 1 mM PMFS, and 0.5% Triton X-100) and lysed by three cycles of freeze-thaw in
589 liquid nitrogen. Lysates were clarified at 4°C by centrifugation at 48,000 x g for 20 min, and
590 incubated with 100 µL of anti-DYKDDDDK (FLAG) resin (Thermo Fisher Scientific) for 2 h at
591 4°C. The resin was washed five times with 200 µL lysis buffer. FLAG-tagged proteins were
592 released from the resin by incubation with buffer supplemented with 50 mM FLAG peptide
593 (Genscript, Piscataway, NJ) for 30 min.
594
595 For boiling and refolding experiments, the proteins purified from the FLAG resin were heated for
596 10 min at 90°C and then allowed to cool to 25°C over 30 min. The proteins were incubated for 2
597 h at 4°C with 100 µL of V5 resin, washed five times with 200 µL lysis buffer, and directly used
598 for analysis. Equal volumes (100 µL) of lysate, flowthrough, 1st wash, last wash, FLAG elution,
599 and V5 resin-bound proteins were mixed with 25 µL of 4x Laemmli SDS-PAGE loading buffer
600 and analyzed by Western blotting using primary FLAG (Santa Cruz Biotechnology, Dallas, TX)
601 and V5 antibodies (Thermo Fisher Scientific). Secondary ECL-linked anti-mouse and anti-rabbit
602 antibodies (Cytiva Life Sciences) were applied and the blots were imaged using a Pierce ECL
603 Plus Western Blotting Substrate (Thermo Fisher Scientific) on a G:BOX Chemi XR5 imager
604 (Syngene, Frederick, MD).
605
606
607 **Acknowledgements**
608
609 This work was supported by National Institutes of Health Grants R01 GM073791 and R01
610 MH087950 to RD and T32 AR053461 to PJC. We thank Pekka Lappalainen for the gift of
611 vectors for the bacterial expression of tropomyosin isoforms. We thank the Quantitative

Proteomics Resource Core at the Perelman School of Medicine (University of Pennsylvania), Hyoungjoo Lee, Joseph Cesare, and Michael Gilbert for help with the proteomics data acquisition and analysis. We thank Michael Shortreed for help with the use of the program MetaMorpheus.

Author contributions

Peter J. Carman: conceptualization, resources, data analysis, validation, investigation, visualization, methodology, project administration, writing and review/editing
Kyle R. Barrie: methodology, review/editing
Roberto Dominguez: conceptualization, supervision, project administration, funding acquisition, writing and review/editing

Author ORCIDs

Peter J. Carman http://orcid.org/0000-0002-6120-5507
Kyle R. Barrie https://orcid.org/0000-0003-0860-1639
Roberto Dominguez https://orcid.org/0000-0003-3186-5229

References

1. Waugh, D. S. (2011) An overview of enzymatic reagents for the removal of affinity tags. *Protein Expr Purif* **80**, 283-293
2. Khoury, G. A., Baliban, R. C., and Floudas, C. A. (2011) Proteome-wide post-translational modification statistics: frequency analysis and curation of the swiss-prot database. *Sci Rep* **1**
3. Bah, A., and Forman-Kay, J. D. (2016) Modulation of Intrinsically Disordered Protein Function by Post-translational Modifications. *J Biol Chem* **291**, 6696-6705
4. Hunter, T. (2009) Tyrosine phosphorylation: thirty years and counting. *Curr Opin Cell Biol* **21**, 140-146
5. Johnson, L. N., and Lewis, R. J. (2001) Structural basis for control by phosphorylation. *Chem Rev* **101**, 2209-2242
6. Walsh, C. T., Garneau-Tsodikova, S., and Gatto, G. J., Jr. (2005) Protein posttranslational modifications: the chemistry of proteome diversifications. *Angew Chem Int Ed Engl* **44**, 7342-7372
7. Amann, T., Schmieder, V., Faustrup Kildegaard, H., Borth, N., and Andersen, M. R. (2019) Genetic engineering approaches to improve posttranslational modification of biopharmaceuticals in different production platforms. *Biotechnol Bioeng* **116**, 2778-2796
8. Brown, C. W., Sridhara, V., Boutz, D. R., Person, M. D., Marcotte, E. M., Barrick, J. E., and Wilke, C. O. (2017) Large-scale analysis of post-translational modifications in E. coli under glucose-limiting conditions. *BMC Genomics* **18**, 301
9. Higel, F., Seidl, A., Sorgel, F., and Friess, W. (2016) N-glycosylation heterogeneity and the influence on structure, function and pharmacokinetics of monoclonal antibodies and Fc fusion proteins. *Eur J Pharm Biopharm* **100**, 94-100
10. McKenzie, E. A., and Abbott, W. M. (2018) Expression of recombinant proteins in insect and mammalian cells. *Methods* **147**, 40-49
11. Tang, H., Wang, S., Wang, J., Song, M., Xu, M., Zhang, M., Shen, Y., Hou, J., and Bao, X. (2016) N-hypermannose glycosylation disruption enhances recombinant protein

663 production by regulating secretory pathway and cell wall integrity in Saccharomyces
664 cerevisiae. *Sci Rep* **6**, 25654
665 12. Weis, B. L., Guth, N., Fischer, S., Wissing, S., Fradin, S., Holzmann, K. H., Handrick, R.,
666 and Otte, K. (2018) Stable miRNA overexpression in human CAP cells: Engineering
667 alternative production systems for advanced manufacturing of biologics using miR-136
668 and miR-3074. *Biotechnol Bioeng* **115**, 2027-2038
669 13. Dunn, A. Y., Melville, M. W., and Frydman, J. (2001) Review: cellular substrates of the
670 eukaryotic chaperonin TRiC/CCT. *J Struct Biol* **135**, 176-184
671 14. Liu, Z., Tyo, K. E., Martinez, J. L., Petranovic, D., and Nielsen, J. (2012) Different
672 expression systems for production of recombinant proteins in Saccharomyces
673 cerevisiae. *Biotechnol Bioeng* **109**, 1259-1268
674 15. Resnicow, D. I., Deacon, J. C., Warrick, H. M., Spudich, J. A., and Leinwand, L. A.
675 (2010) Functional diversity among a family of human skeletal muscle myosin motors.
676 *Proc Natl Acad Sci U S A* **107**, 1053-1058
677 16. Thomas, J. A., and Tate, C. G. (2014) Quality control in eukaryotic membrane protein
678 overproduction. *J Mol Biol* **426**, 4139-4154
679 17. Brault, V., Reedy, M. C., Sauder, U., Kammerer, R. A., Aebi, U., and Schoenenberger,
680 C. (1999) Substitution of flight muscle-specific actin by human (beta)-cytoplasmic actin in
681 the indirect flight muscle of Drosophila. *J Cell Sci* **112 (Pt 21)**, 3627-3639
682 18. Sliwinska, M., Skorzewski, R., and Moraczewska, J. (2008) Role of actin C-terminus in
683 regulation of striated muscle thin filament. *Biophys J* **94**, 1341-1347
684 19. Chant, A., Kraemer-Pecore, C. M., Watkin, R., and Kneale, G. G. (2005) Attachment of a
685 histidine tag to the minimal zinc finger protein of the Aspergillus nidulans gene regulatory
686 protein AreA causes a conformational change at the DNA-binding site. *Protein Expr Purif*
687 **39**, 152-159
688 20. Suh-Lailam, B. B., and Hevel, J. M. (2009) Efficient cleavage of problematic tobacco
689 etch virus (TEV)-protein arginine methyltransferase constructs. *Anal Biochem* **387**, 130-
690 132
691 21. Wu, J., and Filutowicz, M. (1999) Hexahistidine (His6)-tag dependent protein
692 dimerization: a cautionary tale. *Acta Biochim Pol* **46**, 591-599
693 22. Gunning, P. W., Hardeman, E. C., Lappalainen, P., and Mulvihill, D. P. (2015)
694 Tropomyosin - master regulator of actin filament function in the cytoskeleton. *Journal of*
695 *cell science* **128**, 2965-2974
696 23. Geeves, M. A., Hitchcock-DeGregori, S. E., and Gunning, P. W. (2015) A systematic
697 nomenclature for mammalian tropomyosin isoforms. *J Muscle Res Cell Motil* **36**, 147-
698 153
699 24. Meiring, J. C. M., Bryce, N. S., Wang, Y., Taft, M. H., Manstein, D. J., Liu Lau, S., Stear,
700 J., Hardeman, E. C., and Gunning, P. W. (2018) Co-polymers of Actin and Tropomyosin
701 Account for a Major Fraction of the Human Actin Cytoskeleton. *Curr Biol* **28**, 2331-2337
702 e2335
703 25. Gunning, P. W., Ghoshdastider, U., Whitaker, S., Popp, D., and Robinson, R. C. (2015)
704 The evolution of compositionally and functionally distinct actin filaments. *J Cell Sci* **128**,
705 2009-2019
706 26. Lehman, W., Hatch, V., Korman, V., Rosol, M., Thomas, L., Maytum, R., Geeves, M. A.,
707 Van Eyk, J. E., Tobacman, L. S., and Craig, R. (2000) Tropomyosin and actin isoforms
708 modulate the localization of tropomyosin strands on actin filaments. *J Mol Biol* **302**, 593-
709 606
710 27. McKillop, D. F., and Geeves, M. A. (1993) Regulation of the interaction between actin
711 and myosin subfragment 1: evidence for three states of the thin filament. *Biophys J* **65**,
712 693-701

713 28. Cheng, C., Nowak, R. B., Amadeo, M. B., Biswas, S. K., Lo, W.-K., and Fowler, V. M.
714 (2018) Tropomyosin 3.5 protects the F-actin networks required for tissue biomechanical
715 properties. *Journal of cell science* **131**, jcs.222042-jcs.222042
716 29. Pleines, I., Woods, J., Chappaz, S., Kew, V., Foad, N., Ballester-Beltrán, J., Aurbach, K.,
717 Lincetto, C., Lane, R. M., Schevzov, G., Alexander, W. S., Hilton, D. J., Astle, W. J.,
718 Downes, K., Nurden, P., Westbury, S. K., Mumford, A. D., Obaji, S. G., Collins, P. W.,
719 Delerue, F., Ittner, L. M., Bryce, N. S., Holliday, M., Lucas, C. A., Hardeman, E. C.,
720 Ouwehand, W. H., Gunning, P. W., Turro, E., Tijssen, M. R., Kile, B. T., and Kile, B. T.
721 (2017) Mutations in tropomyosin 4 underlie a rare form of human
722 macrothrombocytopenia. *The Journal of clinical investigation* **127**, 814-829
723 30. Kee, A. J., Gunning, P. W., and Hardeman, E. C. (2009) A cytoskeletal tropomyosin can
724 compromise the structural integrity of skeletal muscle. *Cell Motil Cytoskeleton* **66**, 710-
725 720
726 31. Vlahovich, N., Kee, A. J., Van der Poel, C., Kettle, E., Hernandez-Deviez, D., Lucas, C.,
727 Lynch, G. S., Parton, R. G., Gunning, P. W., and Hardeman, E. C. (2009) Cytoskeletal
728 tropomyosin Tm5NM1 is required for normal excitation-contraction coupling in skeletal
729 muscle. *Mol Biol Cell* **20**, 400-409
730 32. Eppinga, R. D., Li, Y., Lin, J. L., and Lin, J. J. (2006) Tropomyosin and caldesmon
731 regulate cytokinesis speed and membrane stability during cell division. *Arch Biochem*
732 *Biophys* **456**, 161-174
733 33. Thoms, J. A., Loch, H. M., Bamburg, J. R., Gunning, P. W., and Weinberger, R. P.
734 (2008) A tropomyosin 1 induced defect in cytokinesis can be rescued by elevated
735 expression of cofilin. *Cell Motil Cytoskeleton* **65**, 979-990
736 34. Hook, J., Lemckert, F., Qin, H., Schevzov, G., and Gunning, P. (2004) Gamma
737 Tropomyosin Gene Products Are Required for Embryonic Development. *Molecular and*
738 *Cellular Biology* **24**, 2318-2323
739 35. Hook, J., Lemckert, F., Schevzov, G., Fath, T., and Gunning, P. (2011) Functional
740 identity of the gamma tropomyosin gene: Implications for embryonic development,
741 reproduction and cell viability. *Bioarchitecture* **1**, 49-59
742 36. Dalby-Payne, J. R., O'Loughlin, E. V., and Gunning, P. (2003) Polarization of specific
743 tropomyosin isoforms in gastrointestinal epithelial cells and their impact on CFTR at the
744 apical surface. *Mol Biol Cell* **14**, 4365-4375
745 37. Dufour, C., Weinberger, R. P., and Gunning, P. (1998) Tropomyosin isoform diversity
746 and neuronal morphogenesis. *Immunology and Cell Biology* **76**, 424-429
747 38. Had, L., Faivre-Sarrailh, C., Legrand, C., and Rabie, A. (1993) The expression of
748 tropomyosin genes in pure cultures of rat neurons, astrocytes and oligodendrocytes is
749 highly cell-type specific and strongly regulated during development. *Brain Res Mol Brain*
750 *Res* **18**, 77-86
751 39. Hannan, A. J., Gunning, P., Jeffrey, P. L., and Weinberger, R. P. (1998) Structural
752 Compartments within Neurons: Developmentally Regulated Organization of
753 Microfilament Isoform mRNA and Protein. *Molecular and Cellular Neuroscience* **11**, 289-
754 304
755 40. Heald, R. W., and Hitchcock-DeGregori, S. E. (1988) The structure of the amino
756 terminus of tropomyosin is critical for binding to actin in the absence and presence of
757 troponin. *J Biol Chem* **263**, 5254-5259
758 41. Palm, T., Greenfield, N. J., and Hitchcock-DeGregori, S. E. (2003) Tropomyosin ends
759 determine the stability and functionality of overlap and troponin T complexes. *Biophys J*
760 **84**, 3181-3189
761 42. Maytum, R., Geeves, M. A., and Konrad, M. (2000) Actomyosin regulatory properties of
762 yeast tropomyosin are dependent upon N-terminal modification. *Biochemistry* **39**, 11913-
763 11920

764 43. Lehman, W., Medlock, G., Li, X. E., Suphamungmee, W., Tu, A. Y., Schmidtmann, A.,
765 Ujfalusi, Z., Fischer, S., Moore, J. R., Geeves, M. A., and Regnier, M. (2015)
766 Phosphorylation of Ser283 enhances the stiffness of the tropomyosin head-to-tail
767 overlap domain. *Arch Biochem Biophys* **571**, 10-15
768 44. Palani, S., Köster, D. V., Hatano, T., Kamnev, A., Kanamaru, T., Brooker, H. R.,
769 Hernandez-Fernaud, J. R., Jones, A. M. E., Millar, J. B. A., Mulvihill, D. P., and
770 Balasubramanian, M. K. (2019) Phosphoregulation of tropomyosin is crucial for actin
771 cable turnover and division site placement. *Journal of Cell Biology* **218**, 3548-3559
772 45. Rajan, S., Jagatheesan, G., Petrashevskaya, N., Biesiadecki, B. J., Warren, C. M.,
773 Riddle, T., Liggett, S., Wolska, B. M., Solaro, R. J., and Wieczorek, D. F. (2019)
774 Tropomyosin pseudo-phosphorylation results in dilated cardiomyopathy. *J Biol Chem*
775 **294**, 2913-2923
776 46. Rao, V. S., Marongelli, E. N., and Guilford, W. H. (2009) Phosphorylation of tropomyosin
777 extends cooperative binding of myosin beyond a single regulatory unit. *Cell Motil*
778 *Cytoskeleton* **66**, 10-23
779 47. Brooker, H. R., Geeves, M. A., and Mulvihill, D. P. (2016) Analysis of biophysical and
780 functional consequences of tropomyosin-fluorescent protein fusions. *FEBS Lett* **590**,
781 3111-3121
782 48. Frye, J., Klenchin, V. A., and Rayment, I. (2010) Structure of the tropomyosin overlap
783 complex from chicken smooth muscle: insight into the diversity of N-terminal recognition.
784 *Biochemistry* **49**, 4908-4920
785 49. Monteiro, P. B., Lataro, R. C., Ferro, J. A., and Reinach Fde, C. (1994) Functional alpha-
786 tropomyosin produced in Escherichia coli. A dipeptide extension can substitute the
787 amino-terminal acetyl group. *J Biol Chem* **269**, 10461-10466
788 50. Johnson, M., Coulton, A. T., Geeves, M. A., and Mulvihill, D. P. (2010) Targeted amino-
789 terminal acetylation of recombinant proteins in E. coli. *PLoS One* **5**, e15801
790 51. Wingfield, P. T. (2017) N-Terminal Methionine Processing. *Curr Protoc Protein Sci* **88**, 6
791 14 11-16 14 13
792 52. Schmid, A. W., Fauvet, B., Moniatte, M., and Lashuel, H. A. (2013) Alpha-synuclein
793 post-translational modifications as potential biomarkers for Parkinson disease and other
794 synucleinopathies. *Mol Cell Proteomics* **12**, 3543-3558
795 53. Zhang, J., Li, X., and Li, J. D. (2019) The Roles of Post-translational Modifications on
796 alpha-Synuclein in the Pathogenesis of Parkinson's Diseases. *Front Neurosci* **13**, 381
797 54. Backliwal, G., Hildinger, M., Hasija, V., and Wurm, F. M. (2008) High-density transfection
798 with HEK-293 cells allows doubling of transient titers and removes need for a priori DNA
799 complex formation with PEI. *Biotechnol Bioeng* **99**, 721-727
800 55. Liu, C., Dalby, B., Chen, W., Kilzer, J. M., and Chiou, H. C. (2008) Transient transfection
801 factors for high-level recombinant protein production in suspension cultured mammalian
802 cells. *Mol Biotechnol* **39**, 141-153
803 56. Shah, N. H., and Muir, T. W. (2014) Inteins: Nature's Gift to Protein Chemists. *Chem Sci*
804 **5**, 446-461
805 57. Southworth, M. W., Amaya, K., Evans, T. C., Xu, M. Q., and Perler, F. B. (1999)
806 Purification of proteins fused to either the amino or carboxy terminus of the
807 Mycobacterium xenopi gyrase A intein. *Biotechniques* **27**, 110-114, 116, 118-120
808 58. Aksnes, H., Drazic, A., Marie, M., and Arnesen, T. (2016) First Things First: Vital Protein
809 Marks by N-Terminal Acetyltransferases. *Trends Biochem Sci* **41**, 746-760
810 59. Gray, D. (2001) Overview of protein expression by mammalian cells. *Curr Protoc Protein*
811 *Sci* **Chapter 5**, Unit5 9
812 60. Khan, K. H. (2013) Gene expression in Mammalian cells and its applications. *Adv Pharm*
813 *Bull* **3**, 257-263

814 61. Tokmakov, A. A., Kurotani, A., Takagi, T., Toyama, M., Shirouzu, M., Fukami, Y., and
815 Yokoyama, S. (2012) Multiple post-translational modifications affect heterologous protein
816 synthesis. *J Biol Chem* **287**, 27106-27116
817 62. Wood, D. W., and Camarero, J. A. (2014) Intein applications: from protein purification
818 and labeling to metabolic control methods. *J Biol Chem* **289**, 14512-14519
819 63. Telenti, A., Southworth, M., Alcaide, F., Daugelat, S., Jacobs, W. R., Jr., and Perler, F.
820 B. (1997) The Mycobacterium xenopi GyrA protein splicing element: characterization of
821 a minimal intein. *J Bacteriol* **179**, 6378-6382
822 64. Hirata, R., Ohsumk, Y., Nakano, A., Kawasaki, H., Suzuki, K., and Anraku, Y. (1990)
823 Molecular structure of a gene, VMA1, encoding the catalytic subunit of H(+)-translocating
824 adenosine triphosphatase from vacuolar membranes of Saccharomyces cerevisiae. *J*
825 *Biol Chem* **265**, 6726-6733
826 65. Kane, P. M., Yamashiro, C. T., Wolczyk, D. F., Neff, N., Goebl, M., and Stevens, T. H.
827 (1990) Protein splicing converts the yeast TFP1 gene product to the 69-kD subunit of the
828 vacuolar H(+)-adenosine triphosphatase. *Science* **250**, 651-657
829 66. Chong, S., Shao, Y., Paulus, H., Benner, J., Perler, F. B., and Xu, M. Q. (1996) Protein
830 splicing involving the Saccharomyces cerevisiae VMA intein. The steps in the splicing
831 pathway, side reactions leading to protein cleavage, and establishment of an in vitro
832 splicing system. *J Biol Chem* **271**, 22159-22168
833 67. Garcia, A., Cayla, X., Guergnon, J., Dessauge, F., Hospital, V., Rebollo, M. P.,
834 Fleischer, A., and Rebollo, A. (2003) Serine/threonine protein phosphatases PP1 and
835 PP2A are key players in apoptosis. *Biochimie* **85**, 721-726
836 68. Sun, H., and Wang, Y. (2012) Novel Ser/Thr protein phosphatases in cell death
837 regulation. *Physiology (Bethesda)* **27**, 43-52
838 69. Van Hoof, C., and Goris, J. (2003) Phosphatases in apoptosis: to be or not to be, PP2A
839 is in the heart of the question. *Biochim Biophys Acta* **1640**, 97-104
840 70. Huyer, G., Liu, S., Kelly, J., Moffat, J., Payette, P., Kennedy, B., Tsaprailis, G., Gresser,
841 M. J., and Ramachandran, C. (1997) Mechanism of inhibition of protein-tyrosine
842 phosphatases by vanadate and pervanadate. *J Biol Chem* **272**, 843-851
843 71. Ishihara, H., Martin, B. L., Brautigan, D. L., Karaki, H., Ozaki, H., Kato, Y., Fusetani, N.,
844 Watabe, S., Hashimoto, K., Uemura, D., and et al. (1989) Calyculin A and okadaic acid:
845 inhibitors of protein phosphatase activity. *Biochem Biophys Res Commun* **159**, 871-877
846 72. Drazic, A., Myklebust, L. M., Ree, R., and Arnesen, T. (2016) The world of protein
847 acetylation. *Biochim Biophys Acta* **1864**, 1372-1401
848 73. Anderson, J. P., Walker, D. E., Goldstein, J. M., de Laat, R., Banducci, K., Caccavello,
849 R. J., Barbour, R., Huang, J., Kling, K., Lee, M., Diep, L., Keim, P. S., Shen, X.,
850 Chataway, T., Schlossmacher, M. G., Seubert, P., Schenk, D., Sinha, S., Gai, W. P., and
851 Chilcote, T. J. (2006) Phosphorylation of Ser-129 is the dominant pathological
852 modification of alpha-synuclein in familial and sporadic Lewy body disease. *J Biol Chem*
853 **281**, 29739-29752
854 74. Hornbeck, P. V., Zhang, B., Murray, B., Kornhauser, J. M., Latham, V., and Skrzypek, E.
855 (2015) PhosphoSitePlus, 2014: mutations, PTMs and recalibrations. *Nucleic Acids Res*
856 **43**, D512-520
857 75. Schey, K. L., and Finley, E. L. (2000) Identification of peptide oxidation by tandem mass
858 spectrometry. *Acc Chem Res* **33**, 299-306
859 76. Gateva, G., Kremneva, E., Reindl, T., Kotila, T., Kogan, K., Gressin, L., Gunning, P. W.,
860 Manstein, D. J., Michelot, A., and Lappalainen, P. (2017) Tropomyosin Isoforms Specify
861 Functionally Distinct Actin Filament Populations In Vitro. *Curr Biol* **27**, 705-713
862 77. Tobacman, L. S. (2008) Cooperative binding of tropomyosin to actin. *Adv Exp Med Biol*
863 **644**, 85-94

78. Wegner, A. (1979) Equilibrium of the actin-tropomyosin interaction. *J Mol Biol* **131**, 839-853
79. Yang, Y. Z., Korn, E. D., and Eisenberg, E. (1979) Cooperative binding of tropomyosin to muscle and Acanthamoeba actin. *J Biol Chem* **254**, 7137-7140
80. Bicer, S., and Reiser, P. J. (2013) Complex tropomyosin and troponin T isoform expression patterns in orbital and global fibers of adult dog and rat extraocular muscles. *J Muscle Res Cell Motil* **34**, 211-231
81. Bronson, D. D., and Schachat, F. H. (1982) Heterogeneity of contractile proteins. Differences in tropomyosin in fast, mixed, and slow skeletal muscles of the rabbit. *J Biol Chem* **257**, 3937-3944
82. Sanders, C., Burtnick, L. D., and Smillie, L. B. (1986) Native chicken gizzard tropomyosin is predominantly a beta gamma-heterodimer. *J Biol Chem* **261**, 12774-12778
83. Muthuchamy, M., Grupp, I. L., Grupp, G., O'Toole, B. A., Kier, A. B., Boivin, G. P., Neumann, J., and Wieczorek, D. F. (1995) Molecular and physiological effects of overexpressing striated muscle beta-tropomyosin in the adult murine heart. *J Biol Chem* **270**, 30593-30603
84. Kast, D. J., and Dominguez, R. (2019) Mechanism of IRSp53 inhibition by 14-3-3. *Nat Commun* **10**, 483
85. Coulton, A., Lehrer, S. S., and Geeves, M. A. (2006) Functional homodimers and heterodimers of recombinant smooth muscle tropomyosin. *Biochemistry* **45**, 12853-12858
86. Jancso, A., and Graceffa, P. (1991) Smooth muscle tropomyosin coiled-coil dimers. Subunit composition, assembly, and end-to-end interaction. *J Biol Chem* **266**, 5891-5897
87. Graceffa, P. (1992) Heat-treated smooth muscle tropomyosin. *Biochim Biophys Acta* **1120**, 205-207
88. Lehrer, S. S., and Qian, Y. (1990) Unfolding/refolding studies of smooth muscle tropomyosin. Evidence for a chain exchange mechanism in the preferential assembly of the native heterodimer. *J Biol Chem* **265**, 1134-1138
89. Heeley, D. H. (2013) Phosphorylation of tropomyosin in striated muscle. *J Muscle Res Cell Motil* **34**, 233-237
90. Ribolow, H., and Barany, M. (1977) Phosphorylation of tropomyosin in live frog muscle. *Arch Biochem Biophys* **179**, 718-720
91. Johnson, P., and Smillie, L. B. (1977) Polymerizability of rabbit skeletal tropomyosin: effects of enzymic and chemical modifications. *Biochemistry* **16**, 2264-2269
92. Schmidt, W., Madan, A., Foster, D. B., and Cammarato, A. (2020) Lysine acetylation of F-actin decreases tropomyosin-based inhibition of actomyosin activity. *J Biol Chem* **295**, 15527-15539
93. Jansen, S., and Goode, B. L. (2019) Tropomyosin isoforms differentially tune actin filament length and disassembly. *Mol Biol Cell* **30**, 671-679
94. Solntsev, S. K., Shortreed, M. R., Frey, B. L., and Smith, L. M. (2018) Enhanced Global Post-translational Modification Discovery with MetaMorpheus. *J Proteome Res* **17**, 1844-1851
95. Moraczewska, J., Greenfield, N. J., Liu, Y., and Hitchcock-DeGregori, S. E. (2000) Alteration of tropomyosin function and folding by a nemaline myopathy-causing mutation. *Biophysical journal* **79**, 3217-3225
96. Rynkiewicz, M. J., Prum, T., Hollenberg, S., Kiani, F. A., Fagnant, P. M., Marston, S. B., Trybus, K. M., Fischer, S., Moore, J. R., and Lehman, W. (2017) Tropomyosin Must Interact Weakly with Actin to Effectively Regulate Thin Filament Function. *Biophys J* **113**, 2444-2451

Table S2. Primers used in this study

Primer name	Primer sequence	Purpose
Primers used to construct vector pJCX4		
a3106g_for a3106g_rev	gagcccctgatgctcctcgtccagatcatcc ggatgatctggacgaggagcatcaggggctc	Removal of SapI site from pEGFPC1
a3316g_for a3316g_rev	tcgccgccaagctcctcagcaatatcacggg cccgtgatattgctgaggagcttggcggcga	Removal of SapI site from pEGFPC1
WPRE_for_xbaI WPRE_rev_mfeI	ttctctagataatcaacctctggattacaaaatttgtgaaagattga ttccaattgatgcggggaggcggc	PCR amplify WPRE
MCS_KO_top MCS_KO_bottom	ccggaggagacaataccggaat ctagattccggtattgtctcct	Removing the pEGFP-C1 MCS
Primers used to construct vector pJC8		
IRES_for_BamHI IRES_rev_BspEI	ttcggatccaattcgcccctctccctccc ttctccggaggttgtggccatattatcatcgtgtttttc	PCR amplify IRES
MCS2_top MCS2_bottom	tcgagtcttgatcactaactagtaataccggtactctgca gagtaccggtattactagttagtgatcaagac	Adding MCS1 into pJC8
MCS2_top MCS2_bottom	ccggatatcccgggatcagatctatcgagctcattt ctagaaatgagctcgatagatctgatcccgggatat	Adding MCS2 into pJC8
Primers used for cloning of Tpm and α-synuclein		
TPM1_for_NotI TPM1_rev_SapI	ttcgcggccgcgccaccatggacgccatcaagaagaagatg ggtggttgctcttccgcacatgttgtttaactccagtaaagtctgatcc	Tpm1.6, Tpm1.7 into pJCX4
TPM1_for_NotI TPM2_rev_SapI	ttcgcggccgcgccaccatggacgccatcaagaagaagatg ggttgctcttccgcacaggttgttgagttccagcagg	Tpm2.1 into pJCX4
TPM3_for_NotI TPM3_rev_SapI	ttcgcggccgcgccaccatggctgggatcaccaccatcg ggttgctcttccgcacatctcattcaggtcaagcagggtctg	Tpm3.1, Tpm3.2 into pJCX4
TPM4_for_NotI TPM4_rev_SapI	ttcgcggccgcgccaccatggccggcctcaactcc ggttgctcttccgcatatacagttaagttcgtttagtgtctgatccag	Tpm4.2 into pJCX4
αSyn_for_NotI αSyn_rev_SapI	ttcgcggccgcatggatgtattcatgaaaggactttcaaag ggttgctcttccgcaggcttcaggttcgtagtcttgatac	α-synuclein into pJCX4
1.6_for_NcoI 1.6_rev_BamHI	ttcccatggacgccatcaagaagaagatg ttcggatcctcacatgttgtttaactccagtaaagtctgatccag	Tpm1.6 into pBAT4
3.1_for_NcoI 3.1_rev_XhoI	ttcccatggctgggatcaccaccatc ttcctcgagtcacatctcattcaggtcaagcagggtctg	Tpm3.1 into pBAT4
TPM3_for_XhoI TPM3_rev_BspEI	ttcctcgagatggctgggatcaccaccatc ttctccggacatctcattcaggtcaagcaggg	Tpm3.1, Tpm3.2 into pJC8 MCS1
TPM3_for_NotI TPM3_rev_NheI	ttcgcggccgcgccaccatggctgggatcaccaccatcg ttcgctagccatctcattcaggtcaagcaggg	Tpm3.1, Tpm3.2 into pJC8 MCS2
TPM3_for_XhoI Tpm3.5_rev_BspE1	ttcctcgagatggctgggatcaccaccatc ttctccggatatagaggtcatgtcattgagggcgtggtccagctcctcgctaatg	Tpm3.5 into pJC8 MCS1
TPM4_for_NotI TPM4_rev_NheI	ttcgcggccgcgccaccatggccggcctcaactcc ttcgctagctatacagttaagttcgtttagtgtctgatccag	Tpm4.2 into pJC8 MCS2
TPM3_for_XhoI Tpm3.5_rev_1 Tpm3.5_rev_2 Tpm3.5_rev_BspEI	ttcctcgagatggctgggatcaccaccatc acttcagtttctgggcatagagctcatcttccaggtcatcaattgtcttttccag gtggtccagctcctcgctaatggccttgtacttcagtttctgggcatagagc ttctccggatatagaggtcatgtcattgagggcgtggtccagctcctcgctaatg	Tpm3.5 overlap extension PCR to generate isoform